Assessing the multidimensional complexity of biodiversity using a globally standardized approach

Authors: Robert M. McElderry[1,2]*, Camille Fournier de Lauriere[1], Charbel El Khoury[1], Priyanka Chaudhary[1], Shivakumara Manu[1], Felix Specker[1], Ian Brettell[1], Johan van den Hoogen[1], Daniel S. Maynard[3], Carolina Bello[1], Lalasia Bialic-Murphy[1], Camille S. Delavaux[1], Daisy H. Dent[1,4,5], Thomas W. Elliott[1,6], Laura G. van Galen[1], Thomas Lauber[1], Andrea Paz[7], Gabriel Smith[1], Leland K. Werden[1], Constantin M. Zohner[1], Thomas W. Crowther[1,6]

Affiliations:

1. Institute of Integrative Biology, ETH Zürich (Swiss Federal Institute of Technology), 8092 Zürich, Switzerland
2. Swiss Federal Institute for Forest, Snow and Landscape Research (WSL), 8903 Birmensdorf, Switzerland
3. Department of Genetics, Evolution, and Environment, University College London, London, UK
4. Smithsonian Tropical Research Institute, Ancon, Panamá, República de Panamá
5. Max Planck Institute of Animal Behavior, Konstanz 78315, Germany
6. Restor Eco AG, 8001 Zürich, Switzerland
7. Département de Sciences Biologiques, Université de Montréal, Montréal, Québec, Canada

Author list footnotes:

* Correspondence: robert.mcelderry@usys.ethz.ch

Highlights

1. The value of nature lies in its complexity.
2. We define a global framework for a holistic measure of the state of nature.
3. Inclusion of microbes and invertebrates is crucial to evaluate biodiversity.
4. Human activity consistently reduces and homogenizes biodiversity worldwide.

Summary

Quantifying biodiversity across the globe is critical for transparent reporting and assessment under the Kunming-Montreal Global Biodiversity Framework. Understanding the complexity of biodiversity requires consideration of the variation of life across genes, species, and ecosystems. Achieving this in a standardized way remains a key challenge for creating an equitable nature positive future. Here, we present the Sustainable Ecology and Economic Development (SEED) framework, which assesses the dimensions that structure biodiversity patterns worldwide (genetics, species, and ecosystems) across plants, animals, and microbial taxa, and consolidates this into a single measure of biocomplexity at every location, relative to a 'reference' ecosystem with minimal human disturbance. We describe the SEED methodology and highlight its features, which include numerous datasets collapsed into nine novel dimensions of biodiversity intactness that are integrated into the SEED biocomplexity index. SEED will continuously integrate new datasets and maps to provide up-to-date estimates of local biocomplexity across the planet, providing a tool for decision makers to assess and improve the global state of nature.

Keywords

Biocomplexity; biodiversity monitoring; biodiversity intactness; state of nature; genetic diversity; species diversity; ecosystem diversity

Abbreviations

SEED	Sustainable Ecology and Economic Development
GBF	Kunming-Montreal Global Biodiversity Framework
GEO BON	Group on Earth Observations Biodiversity Observation Network
EBV	Essential Biodiversity Variable
IUCN	International Union for Conservation of Nature
EII	Ecosystem Integrity Index
BII	Biodiversity Intactness Index
MSA	Mean Species Abundance
HMI	Human Modification Index
PNV	Potential Natural Vegetation

1. Introduction

Every species depends on other species to survive. This vast interdependence means biological diversity is critical for the maintenance of life as we know it. However, humans have historically valued the components of nature we can use for food, timber, and medicine over others[1,2]. The development of markets for these products has incentivized their mass propagation at the expense of other components of biodiversity, driving the oversimplification of biological systems and the loss of the ecosystem services on which we depend[3].

As nature positive policy frameworks and nature markets emerge, it is critical that we learn from past challenges. Mechanisms that value a single aspect of nature – such as carbon sequestration – risk driving the oversimplification of the system[4–7]. This can lead to potentially counterproductive outcomes, like the creation of monocultures of exotic tree species at the expense of local biodiversity[7] and human wellbeing[8]. If political and financial structures are to promote the conservation of natural biodiversity, they must be underpinned by robust, globally standardized monitoring that reflects the full dimensionality of life, across genetic, species and ecosystem levels.

The most prominent guidelines for biodiversity monitoring are described within the Kunming-Montreal Global Biodiversity Framework (GBF)[9], which sets a series of global targets to halt and reverse nature loss by 2030. Key targets in the GBF include protecting areas of high biodiversity importance (Target 1), restoring 30% of degraded areas by 2030 (Target 2), and the headline '30x30' target that aims to conserve 30% of the Earth's surface by 2030 (Target 3). In the financial sector, the GBF requires businesses to disclose their impacts on biodiversity (Target 15), and the Taskforce on Nature-related Financial Disclosures was assembled to provide guidance and outline best practices for nature-related disclosures. At the heart of nature-related disclosures is a measure of the "state of nature" against which impacts, dependencies, risks, and opportunities may be measured[10]. However, it is not yet clear what constitutes a suitable measure of the state of nature.

Over the past decade, a growing number of metrics have been developed to measure and monitor biodiversity across the globe. Biodiversity metrics generally fall into one of two categories based on their dataset and scope: local ground-sourced data (e.g. plot surveys, eDNA, bioacoustics monitors and camera traps), and global remotely-sensed data (e.g. radar and multispectral imagery

from satellites)[11]. Local ground-sourced data provide detailed insights into the diversity of organisms, but the scalability of these assessments are challenging [12,13]. Conversely, remotely-sensed data provide globally-standardized assessments of ecosystem-scale characteristics like forest structure[14] and connectivity[15], but not all aspects of nature can be measured directly from satellites. Many global biodiversity metrics incorporate both ground-sourced and remote-sensed data to offer a balance between local relevance and global scope. To align monitoring efforts, the Group on Earth Observations Biodiversity Observation Network (GEO BON) recently proposed a worldwide system of observation networks[16] and established guidelines for 16 Essential Biodiversity Variables (EBVs)[17,18]. However, we lack a coherent method to consolidate these EBVs and all other biodiversity metrics to derive a unified perspective of the state of nature.

To address the need for a unified, globally standardized measure of biodiversity across all its dimensions, we first review existing global biodiversity metrics that are used to measure the current state of nature and highlight their strengths and weaknesses (Section 2). We then present a new integrative framework (the Sustainable Ecology and Economic Development (SEED) framework) which is designed to consolidate the three primary hierarchical levels that underpin biodiversity – genetic, species, and ecosystem – into a single globally standardized measure of biodiversity intactness, which we call biocomplexity (Section 3). Nature is inherently complex, and biocomplexity is defined as the emergent properties from multiple, often hierarchical levels of interacting factors that "affect, sustain, or are modified by living organisms, including humans"[19]. Recognizing this complexity, we designed the SEED framework so that it can integrate numerous global biodiversity maps and include new maps as they become available. This ensures that policy and market tools will have the most up-to-date information on the state of nature.

2. Current state of global biodiversity measurement

Spatially-explicit biodiversity data products consist of a heterogeneous mix of calculations, model predictions, metrics (standard of measure), and indices (aggregation of multiple indicators). Given our exclusive focus on data products mapped over the globe, we hereafter refer to these products in general as 'maps'. We grouped existing maps into three main organizational levels of ecological systems: within-species genetic diversity, among-species diversity, and ecosystem diversity. Global maps at each level reflect different dimensions of diversity that are essential for a holistic

understanding of biocomplexity across the globe. Although some global maps correspond to a given EBV[20], the EBVs do not consist of a set of spatially-explicit global maps[21]. Their main purpose is to identify the key variables and provide standards on how to measure them[17]. Rather than discussing this detail in depth, we identify the strengths and weaknesses of existing maps and the considerations for including them in a unified measure of biodiversity. We conclude this section with a brief description of a fourth group of maps that represent standardized measures of biodiversity.

2.1 Genetic (within-species) diversity

Genetic diversity (heritable variation) represents variation in the genetic composition of individuals within a species and among populations and is the source for adaptive responses to environmental change[22,23]. There are few global measures of genetic diversity and these are estimated from mitochondrial DNA sequences stored in the National Centre for Biotechnology Information GenBank and the Barcode of Life Database[24–26]. While there are good insights about genetic variation for certain plant[27] and animal species[24–26], we currently lack global predictions of genetic variation for most species on the planet. Among the few taxonomic groups that have been studied, loss of genetic diversity is often correlated with the loss of suitable habitat[28] and reduced abundance[29]. This may suggest that we could use measures of population declines to generate proxy measures of decline in genetic diversity, but this population timeseries data is lacking for the vast majority of organismal groups, except for the 5,200+ species in the Living Planet Database[30]. However, with modern advancements in genetic sequencing technology and widespread usage of barcoding and metabarcoding[31], new data are continually becoming available that will enable the global measurement of genetic diversity across taxonomic groups[23].

2.2 Species, phylogenetic, and functional diversity

Global biodiversity research has traditionally focused on emergent patterns of species richness (the number of unique taxa). However, species diversity also includes phylogenetic (i.e., a measure of evolutionary history[32]) and functional diversity, which can provide a more in-depth understanding of diversity patterns across the globe. Species richness maps are generally created by overlaying several species range maps then summing the number of species per pixel[33–35], which in some cases

130 are then modeled against a set of predictor variables before predicting richness[36–38]. Phylogenetic
131 and functional diversity are calculated using a phylogeny[39] or a functional-trait matrix[40] to quantify
132 the unique contributions from each of the species present at each locality and thus provide
133 information about phylogenetic and functional components of diversity. Whereas a species-rich
134 community may be composed of evolutionarily and functionally redundant species, other species-
135 poor communities may (or may not) have more evolutionarily and functionally divergent species
136 that may contribute unique functions to the community. Therefore, highlighting those communities
137 with particularly rich evolutionary roots and functional traits is key for a holistic measure of
138 biodiversity.

139 Species diversity maps inherit biases from their underlying data sources, which affect their
140 applicability. All global biodiversity databases over-represent some regions and under-represent
141 others, typically with a bias toward developed nations[41]. There are also considerable disparities in
142 taxonomic coverage, with a bias toward larger and more charismatic organisms. For example, the
143 IUCN database, which is the source of many biodiversity maps[24,25,42–45], contains distribution data
144 for over 80% of described vertebrate species and 14% of vascular plants, but only 2% of
145 invertebrate species, which represent the vast majority of animal species diversity. In addition,
146 microbes represent 88% to 99% of all species on Earth[46,47] but are vastly underrepresented, with
147 only 0.4% of known fungi and protists included in the IUCN database. This pattern is now changing
148 due to recent advances in high-throughput sequencing technologies that enable us to observe and
149 quantify microscopic and otherwise cryptic species[48], and the availability of microbial biodiversity
150 maps is expanding exponentially[49–52].

151 Species diversity maps are also limited by their original scope and the underlying models. Until
152 now, most global maps of species diversity were not designed to capture fine-scale patterns in
153 species composition, or the effects of local human disturbance. With a focus on broad-scale
154 biogeographic trends, species diversity models use climatic, edaphic, and topographic variables to
155 predict diversity patterns across environmental gradients. The general lack of human influence in
156 early models may be due in part to the recent emergence of global human modification maps53–56
157 and also due to a paucity of biodiversity data in both heavily degraded and intact landscapes. As a
158 result, species diversity maps have low predictive accuracy for quantifying the impacts of human

disturbance (Figure 1). Furthermore, species diversity maps tend to be temporally static, calculated as an average of observations that can span decades. Additionally, sampling methodologies are taxon and/or habitat specific and may also differ by region and discipline or agency. These complexities make it difficult to harmonize available data and generate well-rounded estimates that scale in space and change over time in response to shifting conditions on the ground.

2.3 Ecosystem diversity

In contrast to genetic and species diversity, which rely heavily on ground-sourced data, ecosystem-level maps provide a more up-to-date view of current conditions because they can be measured directly from satellite imagery, or modeled based on spectral imagery (e.g., radar and multispectral imaging). A wealth of global-scale remote sensing products have been designed to capture information about human modifications[55], land use change[57], canopy cover[58], canopy height[59], above and belowground biomass[60,61], soil respiration[62], habitat heterogeneity[63], leaf area index[64], ecosystem connectivity[65,66], net primary productivity[67] and ecological resilience[68,69]. These ecosystem-level maps can be grouped into three broad categories of biodiversity: ecosystem structure, function[17], or connectivity.

Ecosystem structure, function, and connectivity are emergent properties that arise from the combination of species, landscape physiognomy, climate, and human modifications. For example, the occurrence and extent of mangroves[70] and peatlands[71,72] result from a specific set of conditions, and their structural features are critical to their functional roles. The interplay between living organisms and their environment are also key ecosystem properties, perhaps best exemplified by plant-disperser and plant-fungal associations. Global maps of plant-disperser associations or species interaction networks are not currently available, but progress in this field indicates potential for such maps in the future[73]. The field of plant-fungal associations has produced numerous global maps, which predict such functional features as the relative proportions of nitrogen fixing and arbuscular mycorrhizal or ectomycorrhizal associated plants[74] and the densities of plant fine roots[75] across landscapes, which may affect the intensity of mycorrhizal colonization[75], soil moisture[76] and decomposition rates[77]. These ecosystem properties provide a direct link to measures of ecosystem services[78,79]. Just as the three-dimensional structure of an ecosystem characterizes the environmental context in which species coexist, the spatial arrangement of habitat fragments and

188 species-specific dispersal abilities and limitations determine ecosystem connectivity. Ecosystem
189 connectivity tends to decrease with habitat loss and fragmentation, and both connectivity[80] and
190 fragmentation[81] indices can provide unique insights into the ecological functionality at the
191 landscape-scale[82].

192 2.4 Standardized measures of biodiversity
193 Given the challenges of capturing dynamic changes in ecological diversity at a global scale, few
194 analyses estimate how far the ecological community has diverged from its natural state. Using a
195 database from targeted experiments and local studies spanning disturbance gradients, it is possible
196 to identify how land use changes affect ecological diversity and use these relationships to predict
197 ecological intactness across the globe. Three commonly used global indices are the Ecosystem
198 Integrity Index (EII)[83] by the United Nations Environment Programme World Conservation
199 Monitoring Centre, the Biodiversity Intactness Index (BII)[84,85] by the Natural History Museum in
200 London, and the Mean Species Abundance (MSA)[86] index by the Netherlands Environmental
201 Assessment Agency.

202 The EII includes three components: structure, function, and composition. Ecosystem structure is
203 based on the human modification index (HMI)[55]; ecosystem function is measured by the ratio of
204 actual to potential net primary productivity[67]; and ecosystem composition is measured by the
205 BII[84,87]. For a given location, the EII uses the lowest score of the three components to predict the
206 extent to which any ecosystem has been impacted or altered from its original state. The BII uses a
207 linear model of the impacts of land use and related pressures on two aspects of biodiversity, species
208 abundances and compositional similarity, to estimate the intactness of a community of plants,
209 vertebrates, and invertebrates. The MSA index is conceptually similar to the BII but focuses mainly
210 on species abundance, includes additional human-related pressures, and estimates an average
211 intactness value that is weighted by the land use type and its associated human pressures.

212 The MSA, BII, and EII represent the current state-of-the-art in global biodiversity modeling. Yet,
213 there are two key aspects of diversity that these indices do not capture. First, these indices are fairly
214 limited in taxonomic scope. The BII and EII (and to some degree MSA) are primarily based on the
215 PREDICTS database (Projecting Responses of Ecological Diversity In Changing Terrestrial

Systems)[88], which is valuable for quantifying the impact of land use on biodiversity in different regions of the globe. However, at present, the data coverage of PREDICTS represents a relatively limited taxonomic range, including less than 10% of the described species for most large taxonomic groups like vascular plants and invertebrate animals, and a far smaller proportion for microbes[88,89]. Given that these taxa respond differently to human disturbance and show unique global distribution patterns[90,91], the underrepresentation of important taxa may therefore bias global biodiversity assessments. Second, these indices focus exclusively on species level diversity and do not include genetic diversity or, except for the EII, ecosystem level properties that emerge from the web of interactions among species and their environment.

3. A framework for observing biological complexity on Earth

With the increasing combination of ground-sourced and remotely-sensed data, we are at the beginning of a data revolution in global ecology[92,93]. The exponential growth of global ecological datasets and maps across genetic, species, and ecosystem levels represents exciting new opportunities for our understanding of biodiversity across the planet. Conceptual frameworks that integrate and interpret this growing body of information are essential to generate a holistic understanding of global biocomplexity. Our global understanding of biocomplexity will never be fully complete, as emerging scientific assessments continue to capture novel information. Therefore, it is important to establish flexible and dynamic frameworks that can incorporate new and emerging information as it becomes available.

A key element in new nature-related disclosure frameworks is a vaguely defined measure of the state of nature[10], which would presumably represent the full multidimensional complexity of nature, but for which there is currently no agreed upon metric. To address the need for a unified state of nature metric, we present a more holistic ecological framework (hereafter referred to as SEED) that is designed to represent the multidimensionality of nature by defining nine axes of variation, nested within the three hierarchical levels of diversity: genetics, species (including phylogenetic and functional diversity), and ecosystems (Figure 2). Within the genetic and species levels of variation, we include plants, animals, and microbes. The grouping of microbes to include archaea, bacteria, protists, and fungi could be disaggregated in the future as more information becomes available. Within ecosystems, we distinguish three axes: structure, function, and connectivity.

The SEED framework was designed to be a flexible 'living' index, which is poised to incorporate any new map layers relating to any component of biodiversity as they become available. Thus, the SEED index will continually improve as missing data gaps are filled in and technological advancements improve. Currently, the SEED framework leverages 85 global genetics, species, and ecosystem maps (Figure 2a; Table S1) from the global scientific community Analogous to an ensemble model, this approach minimizes the risk of relying on a single dataset and associated model output to provide a more robust accounting of global biodiversity patterns. The framework generates summary indices for nine axes of biodiversity, and also provides a unified biocomplexity index score that represents the intactness of biocomplexity. We apply the term biocomplexity[19] to set it apart from measures of single biodiversity components, and to highlight the inclusion of multiple hierarchical levels of diversity, which emerge not just from the complex interplay between biological life and the environment, but also from the billions of years of physical and biological evolution on Earth.

To generate truly standardized estimates of biocomplexity across the globe, we estimate the similarity (ranging from zero to one) between the current state of an ecosystem and its potential natural state. We defined the natural state empirically using the HMI to mask our set of biodiversity maps. We then summarize the sets of values in these areas by ecoregion and vegetation type and link these summaries to all pixels of the same ecoregion and vegetation type (Figure 2a-c; Section 3.2). Against this empirical counterfactual landscape, the SEED framework summarizes the intactness (i.e., similarity to natural state) of the multiple underlying biodiversity features in each axis and calculates the mean intactness for all nine axes combined to create a unified score: the SEED biocomplexity index (Figure 2e; Section 3.1). All intactness values range between zero and one, where values near zero represent the near absence of biocomplexity (e.g., an open pit mine or paved area), and one represents an area that is equal to a counterfactual reference state (i.e., a minimally-disturbed ecosystem). The SEED framework therefore offers both a single standardized biocomplexity value for any area of interest and nine intactness indices for each axis of biodiversity, thus allowing the user to unpack this information.

3.1 Integrating dimensions of biodiversity

Consolidating the multiple hierarchical levels of biodiversity into a single value is a critical feature that makes our biocomplexity index generalizable and comprehensible. All available global maps are combined within each of the relevant biodiversity axes (Figure S1), using a multivariate kernel estimator[94] (Eq. 1), and then the mean of these nine axes consolidates this information into a single biocomplexity index.

$$K(\boldsymbol{z}, \boldsymbol{z}_r) = exp[-\delta \|\boldsymbol{w} \circ (\boldsymbol{z} - \boldsymbol{z}_r)\|_1] \quad \text{(Eq. 1)}$$

Here, $\boldsymbol{z}$ is a n-dimensional data vector for a given location, where n represents the number of input maps involved in the calculation. The term $\|\boldsymbol{w}(\boldsymbol{z} - \boldsymbol{z}_r)\|_1$ represents the Manhattan distance, (or ℓ^1 distance), between the data vector $\boldsymbol{z}$ and the mean values for the corresponding reference areas $\boldsymbol{z_r}$ after elementwise multiplication ($\circ$) by the n-dimensional vector, $\boldsymbol{w}$, which contains the normalized weight for each input map. The resulting distance value is then converted into a similarity value, which is bounded by zero and one, by applying the kernel function, K, where δ represents a scaling parameter.

Sensitivity of similarity is set by the scaling parameter, δ, which we set for each biodiversity axis according to two criteria. First, δ must be strictly positive to ensure that the kernel values are bound between zero and one. Second, the similarity values measured by K capture the intactness of nature and should span the full range between zero and one. We set δ to the lowest value that met these criteria, given that increasing values simply shifted the distribution further to the left toward zero intactness (see Supplement S1).

The weight of information is the final key consideration in our kernel estimator. We designed this framework to integrate numerous biodiversity maps, and we test it here with 85 maps (Figure S1; Table S2) – ecosystem structure (29), function (13), and connectivity (1); species diversity of plants (11), microbes (13), and animals (13); and genetic diversity of microbes (2), and animals (2). We reprojected all maps to a common projection (epsg:4326) and spatial resolution (30 arc-seconds, ~926 meters at the equator) using a nearest-neighbor algorithm. The maps we reviewed vary in several aspects: coverage extent, spatial resolution, non-independence from other maps, extrapolation across regional data gaps, and in the degree to which satellite imagery or other

measures of local conditions were integrated. To help control for these differences, we developed a dynamic weighting system to define the normalized weight of each map in a set, represented by $\boldsymbol{w}$ (defined above). We grouped non independent layers to share equal weight, resulting in a short hierarchical structure. We also applied a confidence score and associated decreasing confidence with decreasing weight (see Supplement Table S1 for details). Although we found no global maps of the genetic diversity of plants, we filled in a blank map to test the full framework and set the weight of this map to a very small nonzero number.

We structured the integration of the nine biodiversity axes to be an even-weighted average of the intactness in each dimension. This places genetic, species, and ecosystem level diversity on equal grounds in the integrated index. SEED also offers an index for each biodiversity axis for independent use alongside the integrated index. Even weighting of all dimensions ensures equitability within genetic and species diversity among plants, animals, and microbes, which deviates strongly from the more common case wherein smaller, more cryptic taxa are overlooked in favor of more visible or personable taxa. However, if evidence emerges to suggest a different weighting scheme is more ecologically relevant, our method can be adapted in accordance with the evolving scientific landscape.

In practice, a key challenge is that the availability and quality of available maps is not balanced among axes, which resulted in some axes having higher relative weight and therefore more influence on the overall biocomplexity index (See Supplement S1 for details on how confidence scores affect the relative weights among axes). Identifying the optimal weighting for various levels of biodiversity information remains a key challenge for future biodiversity research as our theoretical understanding of ecological systems evolves.

3.2. Reference area as an empirical counterfactual landscape

To measure the intactness of biocomplexity requires establishing a baseline potential state that can be used for comparison. Here, we used an empirical approach to identify the counterfactual baseline potential state for all biodiversity axes and underlying layers. Specifically, we developed an algorithm that uses the HMI[55] and potential natural vegetation (PNV)[57] to select reference areas for each land cover class within each of the 846 ecoregions[95] on Earth (Figure 2b; Supplement

S1.1).This was done separately for each ecoregion to ensure ecologically relevant comparisons. For each ecoregion, we identify the least impacted areas for each land cover class (from the PNV), using a dynamically-defined upper-limit HMI threshold to ensure a sufficiently large area, enabling representative and robust estimates (see Figure 2 and Supplement S1.1). The mean value ± one standard deviation for each biodiversity feature layer within this *least-impacted area* is used as the estimate of $\boldsymbol{z_r}$ in equation 1, forming the basis for comparing all feature values in all pixels of the same vegetation class within each ecoregion. The maximum allowable upper-limit HMI threshold that was used to identify the counterfactual reference community was defined as areas with a HMI < 0.05.

Although a natural landscape with minimal anthropogenic disturbance is not a universal goal in all scenarios, this minimal-disturbance baseline provides an objective, and replicable benchmark for measuring the state of nature. For example, food security and financial wellbeing are the primary considerations in agricultural settings, while restoration targets in conservation settings may deviate from a fully natural state due to a myriad of ecological and socioeconomic factors and needs, as well as previous alterations to the landscape[96]. Management practices and targets will vary depending on the local situation, and progress toward these targets can be evaluated against local minimal-disturbance benchmarks and other landscapes in similar settings. In these contexts, the SEED index provides a useful tool to benchmark local achievement against a globally-standardized biodiversity metric and enables a standardized assessment of biodiversity improvement in response to management practices[17].

We chose to use minimally modified areas as our counterfactual 'intact' reference community because it involves few a priori assumptions and best reflects our current understanding of diversity patterns across the nine defined dimensions of biocomplexity. As such, this approach provides a contemporary benchmark of the current state of nature. Although a 'historic baseline' approach could also be theoretically used, it raises several philosophical challenges, including the recognition that systems are inherently dynamic and non-static [97]. It also poses significant data limitations, with few existing historic baseline maps for most of the nine dimensions of diversity. While historic reference conditions are the most appropriate for certain scientific inquiries, such as assessing nitrogen deposition or climate change, they become less applicable for evaluating more direct

human impacts like mining or agriculture, or for informing conservation and restoration efforts. In such cases, the concept of a historic 'natural' state is more ambiguous. Given these challenges, the counterfactual reference community approach provides a robust and practical framework for characterizing biocomplexity. It avoids overreliance on incomplete historical data and allows for a more comprehensive representation of current diversity across multiple dimensions.

3.3. Illustration of the SEED biocomplexity framework

The biocomplexity framework was developed using a comprehensive list of the most up-to-date global-scale maps of genetic, species, and ecosystem diversity (see Supplement Figure S1 and Table S2). Although, our framework is designed to integrate nine biodiversity axes, the current lack of global maps to represent the genetic diversity of plants limits the current index to eight functioning axes. To illustrate the capabilities of the framework, we first show the viability of our dimensionality reduction calculation (equation 1) and reference area (Figure 2) approach to calculate the intactness of nine biodiversity axes (Figure 3a-h). Combined, these intactness layers generate a unified measure of the intactness of nature, the SEED biocomplexity index (Figure 4a). We show how SEED can be aggregated across ecological boundaries and at various spatial scales to summarize biocomplexity in total and along each biodiversity axis (Figure 4b-c). Finally, we conduct a cursory comparison of SEED against the leading biodiversity intactness indices (Figure S2).

Among the eight (out of nine) biodiversity intactness indices that we calculated, we identified broad global patterns where the indices unanimously show similar levels of intactness (Figure 3). High intactness is nearly universally indicated across tundra, northern boreal forests, deserts, and the Amazon basin – areas that have not experienced extensive human development. Low intactness is indicated in Central and Eastern North America, Brazil's Atlantic Forest, narrow bands along the West African coast and Sub-Saharan Africa, temperate forests across Europe and east across Asia toward Siberia, Northern India, the western edge of Southeast Asia, Northeastern China, and the eastern and southwestern coasts of Australia.

There is also notable divergence among these indices. While the intactness of ecosystem structure (Figure 3b) and ecosystem function (Figure 3d) are larger similar in some regions, these indices

strongly diverge from plant diversity, e.g., parts of North America (northeast and Appalachia) and the Brazilian Cerrado. Within these regions, high intactness of ecosystem function and structure were associated with low intactness of plant diversity. While the factors underpinning these differences remain unclear – it does highlight that examining single components of biodiversity can lead to a skewed perspective when evaluating a system's intactness. This highlights the benefit in using an integrative approach, such as SEED, that combines these axes of diversity into a single measure of biocomplexity; minimizing the risk of valuing some aspects of diversity over others (e.g., ecosystem function versus plant diversity).

The intactness of plant, animal, and microbial species diversity (Figure 3h) also diverge in many regions of the world, with the most prominent differences between the intactness of microbial diversity relative to both plant and animal diversity. While the mechanisms underpinning this emergent pattern remain unclear, it does suggest a decoupling in the intactness of these components of diversity and highlight an exciting avenue for future research.

Ecosystem connectivity (Figure 3c) also appears to form a unique pattern relative to the other indices. However, the SEED connectivity index is highly sensitive to fragmentation[81], and therefore scores land area as either highly intact or highly degraded, highlighting the need for improvements in fragmentation maps. The genetic diversity of animals (Figure 3e) also shows a unique pattern, but this is likely because we have only two genetic diversity maps with very coarse resolution (~380-km)[25]. This, along with the absence of global models for plant genetic diversity, emphasizes the need for future research to prioritize global genetic diversity assessments before they can be equally represented within biocomplexity assessments.

The value in our biocomplexity framework is twofold; it integrates information regarding multiple hierarchical levels of diversity and numerous maps within each level, and it can be aggregated to provide summary statistics at the desired scale. The integrated SEED biocomplexity index represents a single measure of the state of nature for terrestrial land areas across the globe (Figure 4a). This suggests that, on average, the Earth is currently at approximately 60% of its natural ecological state across the three major dimensions of biodiversity (Figure 4b). By aggregating

within administrative boundaries[98], we can evaluate the state of nature at a level where local policies may directly affect the mechanisms governing the direct human impacts on nature (Figure 4c).

In comparison to existing global biodiversity indices, SEED (Figure 4) offers a more comprehensive view of nature's state due to its inclusion of 85 global biodiversity maps, while also offering disaggregated information in the form of nine intactness sub-indices (Figure 3a-h). Existing global intactness indices (BII, and MSA) exclusively represent species level diversity for a subset of taxa. SEED expands the taxa represented with a wealth of microbial datasets (including fungi, bacteria, and archaea), while also expanding in scope to include multiple ecosystem attributes that capture landscape dynamics and ecological feedback. Their inclusion in SEED may account for differences between SEED and the other intactness indices (Figure S2). For example, SEED may indicate low ecosystem intactness where satellite imagery detects ecosystem fragmentation, while models predicting species composition may not register a change in species intactness. Given the global coverage and high temporal resolution of satellite imagery, the inclusion of remote-sensed ecosystem characteristics not only adds dimensionality to biodiversity estimates, but it also improves the spatial and temporal resolution of biodiversity intactness predictions.

While the SEED framework offers the most holistic estimate of biocomplexity to date—drawing on the most comprehensive set of genetic, species, and ecosystem-level data layers—several important caveats remain. These include limited data on the genetic diversity of plants, animals, and microbes, as well as propagated uncertainty of species diversity maps due to unbalanced sampling efforts in under-studied regions of the world. We emphasize that these limitations represent both major conceptual challenges and key opportunities for future research. Addressing these knowledge gaps will improve our understanding of nature’s biocomplexity, which is essential for guiding global biodiversity policy and ensuring financial accountability of market-based nature impacts.

3.4. Spatial and temporal scalability and next steps

There is a growing demand for spatial and temporal scalability in global biodiversity monitoring but achieving this remains a central challenge for ecology. Determining how biodiversity scales in space and time has been the focus of countless investigations, and one general result is that

outcomes are highly context dependent. Meeting the demand for scalability will require reimagining our approach to biodiversity modeling. Work by Map of Life[99] in association with GEO BON exemplifies the scalable biodiversity models of the future. Map of Life provides a catalog of species distributions predicted over space and time, generated using the most up-to-date remote sensing technologies and species distribution models[20]. Bringing these maps together, we can reevaluate species richness, phylogenetic and functional diversity, and genetic diversity via declines in species ranges; and we can generate time series for these biodiversity metrics in high spatial resolution. As these new products emerge, they will be fed directly into the SEED framework to update the biocomplexity index and improve the spatial and temporal resolution of the index to allow for more fine-scale assessments of biodiversity and dynamic changes over time.

The integration of remote sensing in biodiversity modeling will be the key distinguishing factor that transforms novel approaches from simply predicting general patterns to the prediction of local conditions and the actual state of nature. Overall, we gain more complete spatial coverage from remote sensing than would be possible from field observation, with more reliable information than extrapolation of models[100]. Remote sensing can provide the means for both direct – many trees and large animals are visible from space – and indirect biodiversity monitoring via the coupling of remote sensing products with ecological models[101]. Future advances in remote sensing such as hyper-spectral imaging[102,103] are expected to provide valuable additional information, which may help assess how plant species and functional biodiversity respond to different practices[104].

Global biodiversity monitoring undoubtedly requires a combination of ground-sourced and remote-sensed approaches. Future on-the-ground sampling in under-sampled regions of the planet and for under-sampled taxa like invertebrates is urgently needed to fill in key gaps and narrow the uncertainty in global genetic and species diversity models. The emergence of new technologies – such as eDNA[48,105], bioacoustics[106], and camera traps – will likely be essential for filling in these core data gaps in a cost-effective manner[107].

4. Conclusion and outlook

There is growing recognition that we need both the political and financial mechanisms to distribute wealth towards local efforts that promote biodiversity[108]. To support this transition to equitable

biodiversity protection, we require globally standardized assessments of ecological intactness that can detect change over time and are available to everyone, everywhere. Given the expansion of global datasets, across various dimensions of biodiversity including plants, animals, and microbes, frameworks for integrating this information are now within our grasp. The resulting global assessments of biocomplexity are necessary to evaluate progress toward climate change and land protection pledges (e.g. the GBF, Bonn Challenge[109], and UN Sustainable Development Goals[110]) to bring transparency to policy frameworks, and to encourage corporate accountability (e.g., under the Taskforce for Nature-related Financial Disclosures (TNFD)[10] and Science-Based Targets for Nature (SBTN)[111]).

The SEED framework consolidates the three broadest dimensions of biodiversity to produce a single, standardized and comprehensible measure of biocomplexity across the globe. This framework is fundamentally collaborative, incorporating biodiversity assessments and models from a diverse range of biodiversity experts. In addition, it is flexible, allowing for a dynamic index that evolves alongside the development of new map products and scientific advancements. We demonstrate that the SEED framework captures multidimensional changes in biodiversity along nine distinct axes (Figures 3) and provides a unified understanding of the state of nature at multiple scales (Figure 4). Yet, there are several key challenges that need to be addressed to improve the resolution of our index at finer spatial and temporal scales. Most notably, the development of models that integrate remote sensing data products into maps of species richness and genetic diversity will greatly improve the spatial and temporal resolution of our index.

To ensure that the most high-integrity and up-to-date ecological information is available to policy- and decision-makers, we invite the wider scientific community to collaborate on the continual advancement of this biocomplexity index (www.seed-index.com). We believe that for this biodiversity index to lead to positive outcomes, its satellite-based predictions must accurately represent the actual biodiversity at a site. Achieving this level of accuracy presents a scientific challenge that requires the collaboration of a diverse team of experts, including ecologists, remote-sensing specialists, and others from around the globe. Leveraging the latest scientific and technological breakthroughs, we aim to enhance and refine the biocomplexity index, thus fostering better outcomes for ecosystem protection and restoration.

Figures

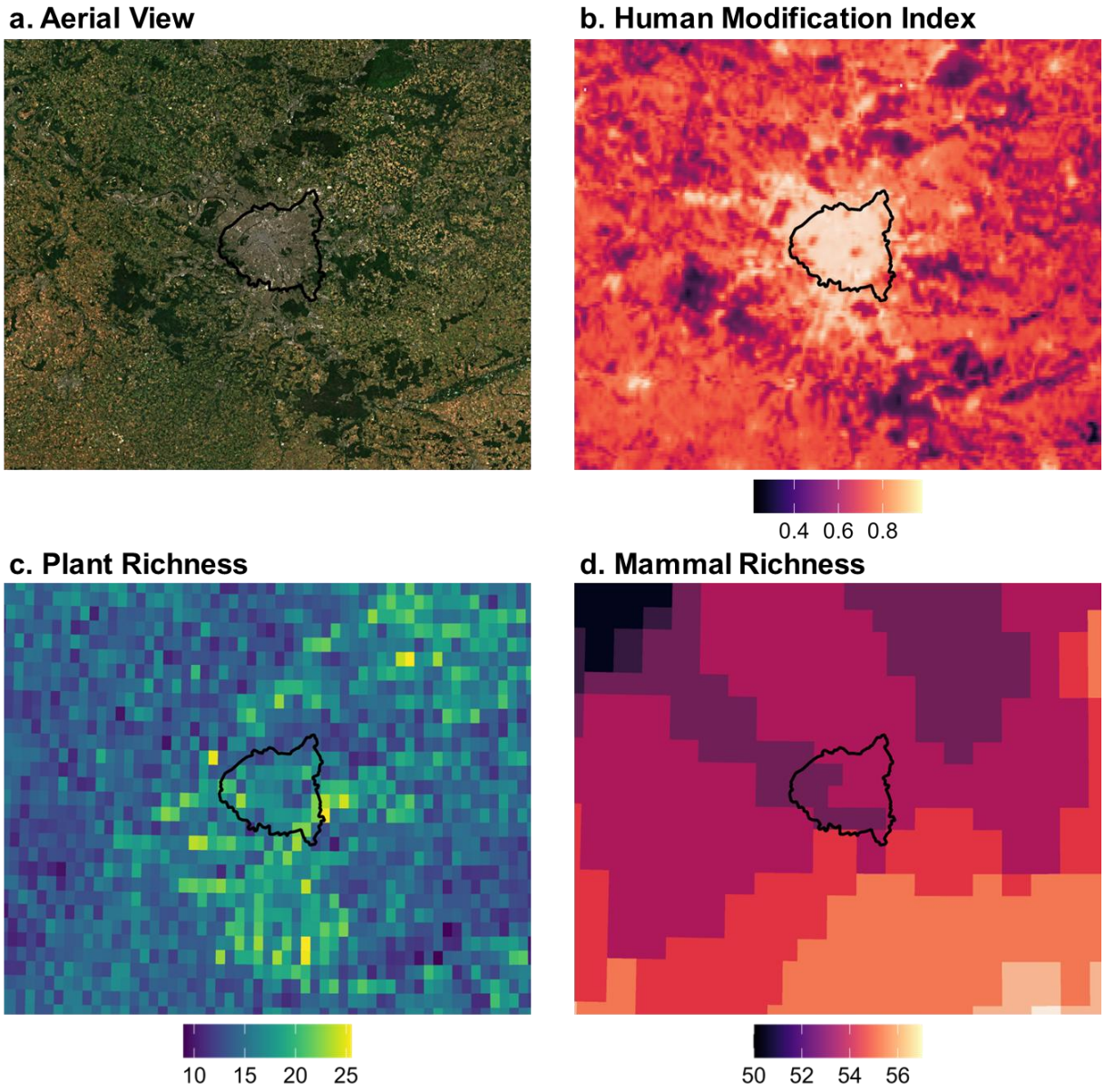

Figure 1. Poor performance of species richness maps in human modified landscapes. The impacts of human activities – as is shown here for Paris (outline) and the surrounding landscape (a) in satellite imagery[112] and (b) in the human modification index[55] – were not included in the development of most maps of species richness, e.g., (c) plant[113] and (d) mammals[34].

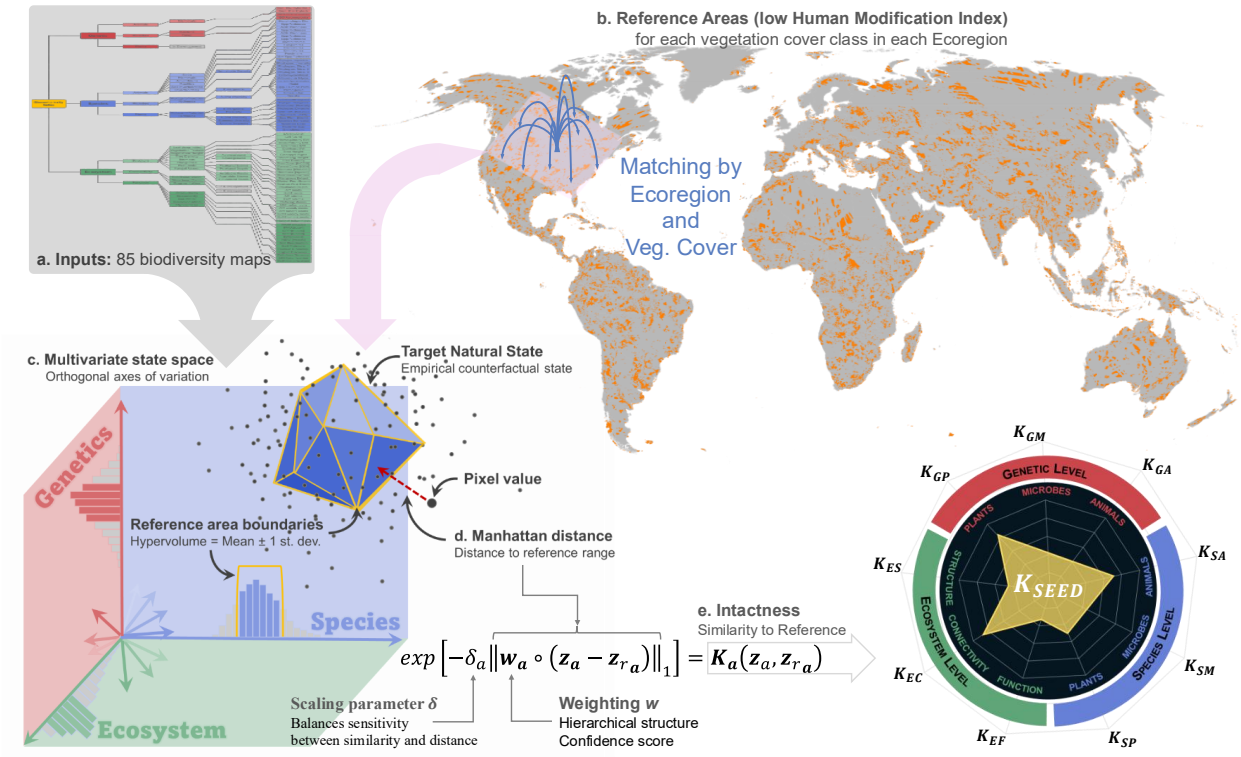

Figure 2. **SEED framework methodology.** (a) We defined a hierarchy to guide the flow of data from 85 biodiversity input layers to each of the nine dimensions of biocomplexity (Figure S1). (b) Using minimally human modified areas to serve as reference points, we linked all pixels to a reference area with matching ecoregion and vegetation class. (c) In a multivariate context, we calculate the bounds for each input as the mean +- one standard deviation. (d) Within each dimension we calculate the Manhattan distance between each pixel and the bounds of the reference area values. (e) The kernel function converts distance to similarity for each of nine dimensions (a E (GP, GM, GA, SP, SM, SA, ES, EC, EF). Similarity to natural reference state indicates intactness, which can be visualized together in the radar plot in yellow. The weighted sum of the nine kernels yields a single biocomplexity intactness index.

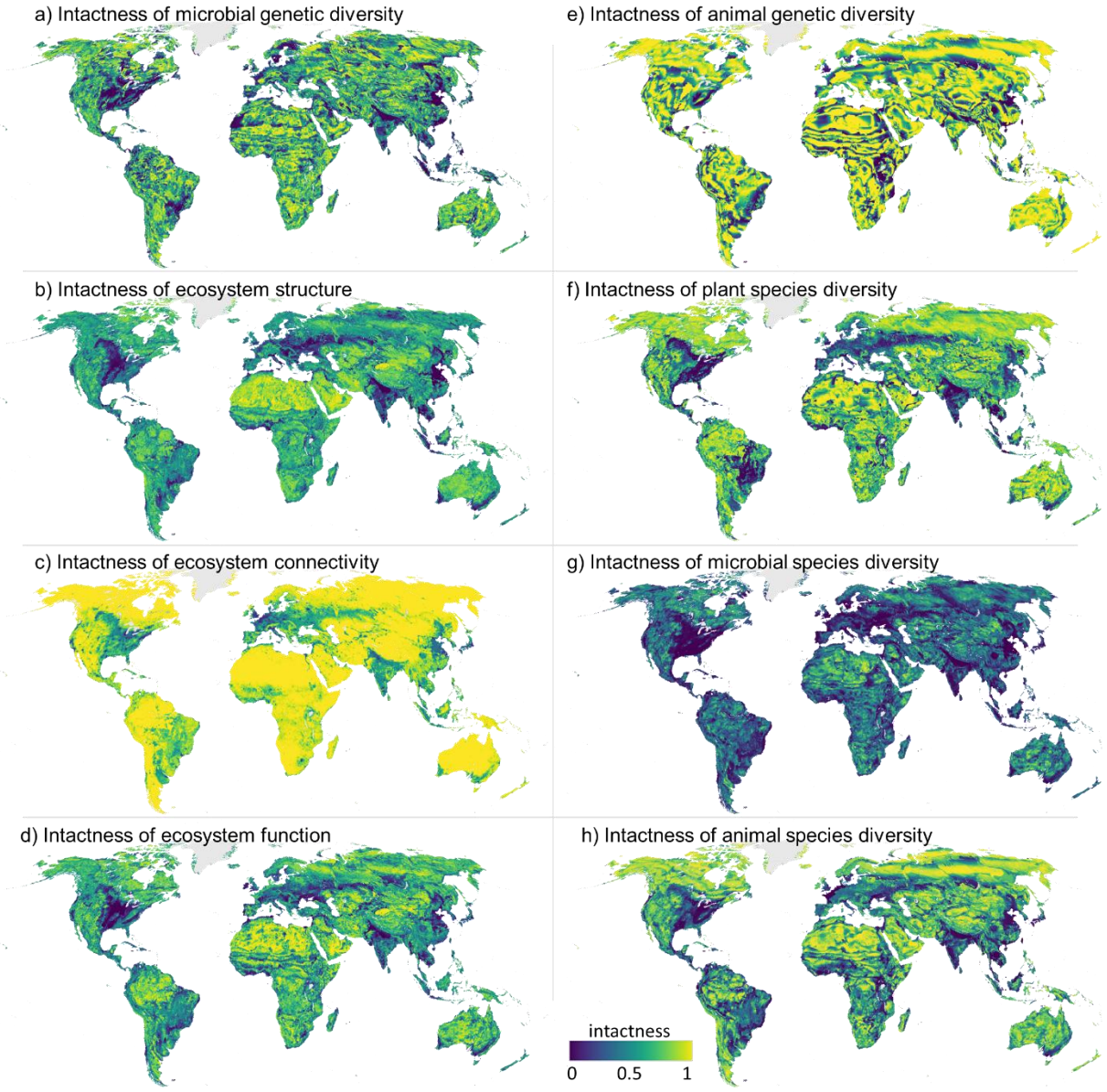

516

517 **Figure 3. Intactness along each axis of biodiversity.** Series of maps showing the intactness –
518 relative to minimally impacted reference areas – of diversity along each biodiversity axis: genetic
519 diversity of (a) microbes and (e) animals; ecosystem (b) structure, (c) connectivity, and (d) function;
520 and species diversity of (f) plants, (g) microbes, and (h) animals.

521

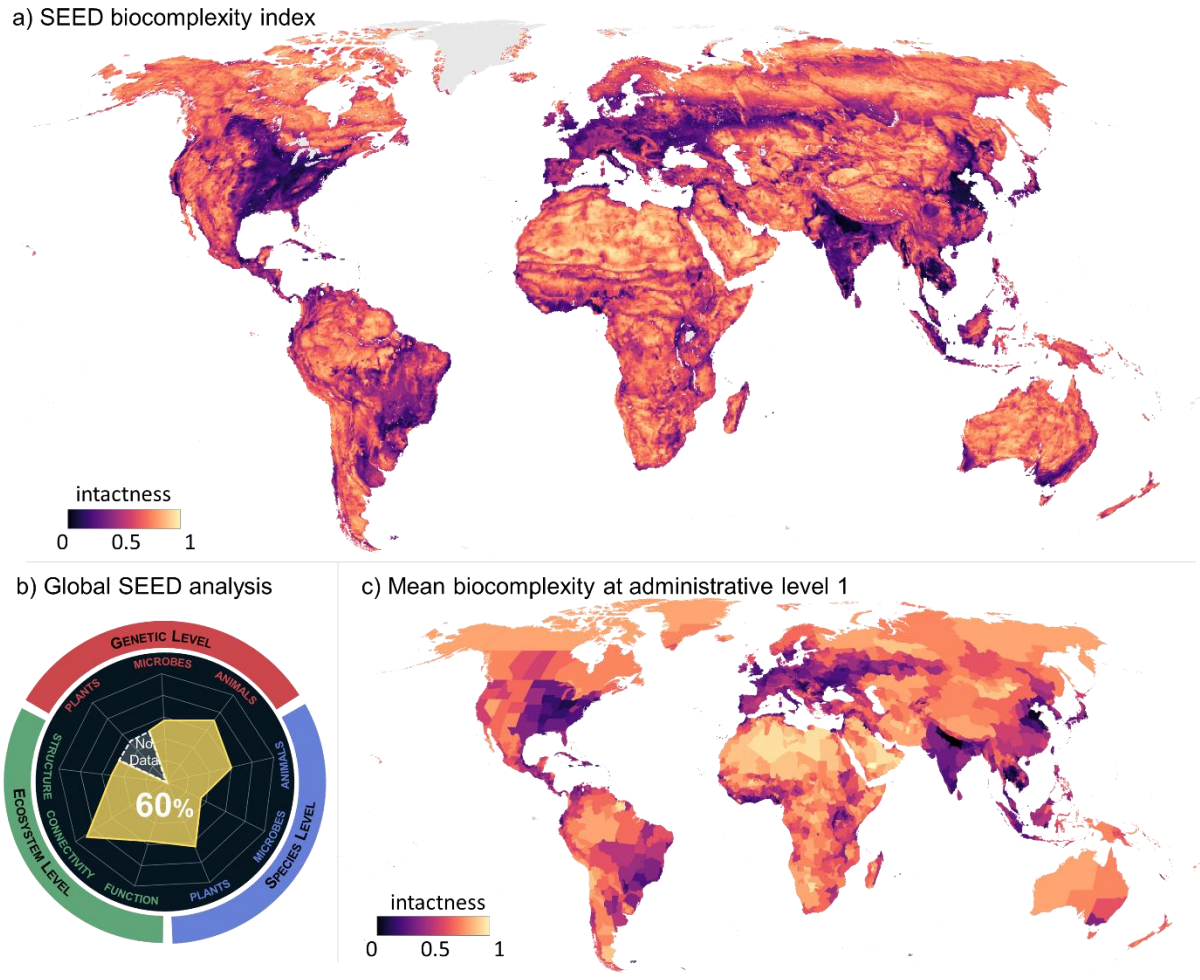

522

523 **Figure 4. Global analysis of biocomplexity.** Map of the (a) SEED biocomplexity index, which
524 measures the intactness of biodiversity for every 1-km of pixel of land. SEED can be aggregated
525 across ecological boundaries, as is demonstrated with (b) a global analysis and (c) the summaries
526 by administrative boundaries.

527

Resource availability

Lead contact: Requests for further information and resources should be directed to and will be fulfilled by the lead contact, Robert McElderry (robert.mcelderry@usys.ethz.ch).

Materials availability: All unique biodiversity indices generated in this study may be accessed at https://doi.org/10.5281/zenodo.13799961

Data and code availability: This paper analyzes existing, publicly available data. We compiled a list of the sources where these data may be accessed [See Excel file]. All original code is currently unavailable.

Acknowledgements:

This work was supported by DOB Ecology, the Bernina Initiative, and Nestlé. CSD was supported by SNSF Postdoctoral fellowship TMPFP3_209925. DHD and LKW were supported by a Google Carbon Removal Research award. We also thank Jelle P. Hilbers for reviewing our manuscript and offering several useful suggestions.

Author contributions:

This work was conceptualized by TWC, DM, JvdH, TE, RMM, and CFL. RMM, CFL, CEL, FS, PC, TWC, and JvdH developed the methodology while CEL, FS, PC, RMM, TL, CFL, and JvdH composed the software. Data curation, formal analyses, and validation were performed by RMM and CFL with assistance from CEL, SM, PC, JvdH and TL. Resources were curated by TL, CFL, CEL, PC, and RMM. The original draft was composed by TWC, RMM, CFL, and IB, followed by revisions by all authors. Visuals were envisioned by TWC, RMM, and IB, and created by CFL and RMM. TWC and RMM supervised this work, and funding was acquired by TWC, TWE, RMM, LKW, and IB.

Declaration of interests:

Restor (Restor Eco AG) is a non-profit spin-out from the Crowther Lab at ETH Zurich and is wholly owned and financed by the Restor Foundation. None of the authors own any shares in Restor. TWE is the CEO of Restor and TCW is the President of the Council of the Restor Foundation and a member of Restor's Science Advisory Council.

Supplemental information:

Document S1. Materials and methods, Table S1-2, and Figure S1-2

Table S2. Citations and details for the list of layers incorporated in SEED. See Excel file.

Web-based map viewer. https://robertmcelderry.users.earthengine.app/view/seed-biocomplexity-global-beta

6. References:

1. Henle, K., Alard, D., Clitherow, J., Cobb, P., Firbank, L., Kull, T., McCracken, D., Moritz, R.F.A., Niemelä, J., Rebane, M., et al. (2008). Identifying and managing the conflicts between agriculture and biodiversity conservation in Europe–A review. Agric. Ecosyst. Environ. *124*, 60–71. https://doi.org/10.1016/j.agee.2007.09.005.

2. Lécuyer, L., Alard, D., Calla, S., Coolsaet, B., Fickel, T., Heinsoo, K., Henle, K., Herzon, I., Hodgson, I., Quétier, F., et al. (2021). Conflicts between agriculture and biodiversity conservation in Europe: Looking to the future by learning from the past. In Advances in Ecological Research (Elsevier), pp. 3–56. https://doi.org/10.1016/bs.aecr.2021.10.005.

3. Lockwood, J.L., and McKinney, M.L. eds. (2001). Biotic Homogenization (Springer US) https://doi.org/10.1007/978-1-4615-1261-5.

4. Bremer, L.L., and Farley, K.A. (2010). Does plantation forestry restore biodiversity or create green deserts? A synthesis of the effects of land-use transitions on plant species richness. Biodivers. Conserv. *19*, 3893–3915. https://doi.org/10.1007/s10531-010-9936-4.

5. Armenteras, D., Rodríguez, N., and Retana, J. (2015). National and regional relationships of carbon storage and tropical biodiversity. Biol. Conserv. *192*, 378–386. https://doi.org/10.1016/j.biocon.2015.10.014.

6. Lima, T.A., and Vieira, G. (2013). High plant species richness in monospecific tree plantations in the Central Amazon. For. Ecol. Manag. *295*, 77–86. https://doi.org/10.1016/j.foreco.2013.01.006.

7. Barlow, J., Gardner, T.A., Araujo, I.S., Ávila-Pires, T.C., Bonaldo, A.B., Costa, J.E., Esposito, M.C., Ferreira, L.V., Hawes, J., Hernandez, M.I.M., et al. (2007). Quantifying the biodiversity value of tropical primary, secondary, and plantation forests. Proc. Natl. Acad. Sci. *104*, 18555–18560. https://doi.org/10.1073/pnas.0703333104.

8. Hulvey, K.B., Hobbs, R.J., Standish, R.J., Lindenmayer, D.B., Lach, L., and Perring, M.P. (2013). Benefits of tree mixes in carbon plantings. Nat. Clim. Change *3*, 869–874. https://doi.org/10.1038/nclimate1862.

9. Conference of the Parties to the Convention on Biological Diversity (2022). Decision 15/4.

10. TNFD – Taskforce on Nature-related Financial Disclosures TNFD. https://tnfd.global/.

11. Geller, G.N., Halpin, P.N., Helmuth, B., Hestir, E.L., Skidmore, A., Abrams, M.J., Aguirre, N., Blair, M., Botha, E., Colloff, M., et al. (2017). Remote Sensing for Biodiversity. In The GEO Handbook on Biodiversity Observation Networks, M. Walters and R. J. Scholes, eds. (Springer International Publishing), pp. 187–210. https://doi.org/10.1007/978-3-319-27288-7_8.

12. Witmer, G.W. (2005). Wildlife population monitoring: some practical considerations. Wildl. Res. *32*, 259–263. https://doi.org/10.1071/WR04003.

13. Adam, E., Mutanga, O., and Rugege, D. (2010). Multispectral and hyperspectral remote sensing for identification and mapping of wetland vegetation: a review. Wetl. Ecol. Manag. *18*, 281–296. https://doi.org/10.1007/s11273-009-9169-z.

14. LaRue, E.A., Fahey, R.T., Alveshere, B.C., Atkins, J.W., Bhatt, P., Buma, B., Chen, A., Cousins, S., Elliott, J.M., Elmore, A.J., et al. (2023). A theoretical framework for the ecological role of three-dimensional structural diversity. Front. Ecol. Environ. *21*, 4–13. https://doi.org/10.1002/fee.2587.

15. Bishop-Taylor, R., Tulbure, M.G., and Broich, M. (2018). Evaluating static and dynamic landscape connectivity modelling using a 25-year remote sensing time series. Landsc. Ecol. *33*, 625–640. https://doi.org/10.1007/s10980-018-0624-1.

16. Gonzalez, A., Vihervaara, P., Balvanera, P., Bates, A.E., Bayraktarov, E., Bellingham, P.J., Bruder, A., Campbell, J., Catchen, M.D., Cavender-Bares, J., et al. (2023). A global biodiversity observing system to unite monitoring and guide action. Nat. Ecol. Evol., 1–5. https://doi.org/10.1038/s41559-023-02171-0.

17. Pereira, H.M., Ferrier, S., Walters, M., Geller, G.N., Jongman, R.H.G., Scholes, R.J., Bruford, M.W., Brummitt, N., Butchart, S.H.M., Cardoso, A.C., et al. (2013). Essential Biodiversity Variables. Science *339*, 277–278. https://doi.org/10.1126/science.1229931.

18. Walters, M., and Scholes, R.J. eds. (2017). The GEO Handbook on Biodiversity Observation Networks (Springer International Publishing) https://doi.org/10.1007/978-3-319-27288-7.

19. Michener, W.K., Baerwald, T.J., Firth, P., Palmer, M.A., Rosenberger, J.L., Sandlin, E.A., and Zimmerman, H. (2001). Defining and Unraveling Biocomplexity. BioScience *51*, 1018. https://doi.org/10.1641/0006-3568(2001)051[1018:DAUB]2.0.CO;2.

20. Jetz, W., McGeoch, M.A., Guralnick, R., Ferrier, S., Beck, J., Costello, M.J., Fernandez, M., Geller, G.N., Keil, P., Merow, C., et al. (2019). Essential biodiversity variables for mapping and monitoring species populations. Nat. Ecol. Evol. *3*, 539–551. https://doi.org/10.1038/s41559-019-0826-1.

21. Peterson, A.T., and Soberón, J. (2018). Essential biodiversity variables are not global. Biodivers. Conserv. *27*, 1277–1288. https://doi.org/10.1007/s10531-017-1479-5.

22. O'Brien, D., Laikre, L., Hoban, S., Bruford, M.W., Ekblom, R., Fischer, M.C., Hall, J., Hvilsom, C., Hollingsworth, P.M., Kershaw, F., et al. (2022). Bringing together approaches to reporting on within species genetic diversity. J. Appl. Ecol. *59*, 2227–2233. https://doi.org/10.1111/1365-2664.14225.

23. Hoban, S., Archer, F.I., Bertola, L.D., Bragg, J.G., Breed, M.F., Bruford, M.W., Coleman, M.A., Ekblom, R., Funk, W.C., Grueber, C.E., et al. (2022). Global genetic diversity status and trends: towards a suite of Essential Biodiversity Variables (EBVs) for genetic composition. Biol. Rev. *97*, 1511–1538. https://doi.org/10.1111/brv.12852.

24. Miraldo, A., Li, S., Borregaard, M.K., Flórez-Rodríguez, A., Gopalakrishnan, S., Rizvanovic, M., Wang, Z., Rahbek, C., Marske, K.A., and Nogués-Bravo, D. (2016). An Anthropocene map of genetic diversity. Science *353*, 1532–1535. https://doi.org/10.1126/science.aaf4381.

25. Theodoridis, S., Fordham, D.A., Brown, S.C., Li, S., Rahbek, C., and Nogues-Bravo, D. (2020). Evolutionary history and past climate change shape the distribution of genetic diversity in terrestrial mammals. Nat. Commun. *11*, 2557. https://doi.org/10.1038/s41467-020-16449-5.

26. French, C.M., Bertola, L.D., Carnaval, A.C., Economo, E.P., Kass, J.M., Lohman, D.J., Marske, K.A., Meier, R., Overcast, I., Rominger, A.J., et al. (2023). Global determinants of insect mitochondrial genetic diversity. Nat. Commun. *14*, 5276. https://doi.org/10.1038/s41467-023-40936-0.

27. Wesse, C., Welk, E., Hurka, H., and Neuffer, B. (2021). Geographical pattern of genetic diversity in Capsella bursa-pastoris (Brassicaceae)—A global perspective. Ecol. Evol. *11*, 199–213. https://doi.org/10.1002/ece3.7010.

28. Exposito-Alonso, M., Booker, T.R., Czech, L., Gillespie, L., Hateley, S., Kyriazis, C.C., Lang, P.L.M., Leventhal, L., Nogues-Bravo, D., Pagowski, V., et al. (2022). Genetic diversity loss in the Anthropocene. Science *377*, 1431–1435. https://doi.org/10.1126/science.abn5642.

29. Canteri, E., Fordham, D.A., Li, S., Hosner, P.A., Rahbek, C., and Nogués-Bravo, D. (2021). IUCN Red List protects avian genetic diversity. Ecography *44*, 1808–1811. https://doi.org/10.1111/ecog.05895.

30. Ledger, S.E.H., Loh, J., Almond, R., Böhm, M., Clements, C.F., Currie, J., Deinet, S., Galewski, T., Grooten, M., Jenkins, M., et al. (2023). Past, present, and future of the Living Planet Index. Npj Biodivers. *2*, 12. https://doi.org/10.1038/s44185-023-00017-3.

31. Adamowicz, S.J., and Steinke, D. (2015). Increasing global participation in genetics research through DNA barcoding. Genome *58*, 519–526. https://doi.org/10.1139/gen-2015-0130.

32. Faith, D.P. (1992). Conservation evaluation and phylogenetic diversity. Biol. Conserv. *61*, 1–10. https://doi.org/10.1016/0006-3207(92)91201-3.

659 33. Graham, C.H., and Hijmans, R.J. (2006). A comparison of methods for mapping species
660 ranges and species richness. Glob. Ecol. Biogeogr. *15*, 578–587.
661 https://doi.org/10.1111/j.1466-8238.2006.00257.x.

662 34. Jenkins, C.N., Pimm, S.L., and Joppa, L.N. (2013). Global patterns of terrestrial vertebrate
663 diversity and conservation. Proc. Natl. Acad. Sci. *110*, E2602–E2610.
664 https://doi.org/10.1073/pnas.1302251110.

665 35. Roll, U., Feldman, A., Novosolov, M., Allison, A., Bauer, A.M., Bernard, R., Böhm, M.,
666 Castro-Herrera, F., Chirio, L., Collen, B., et al. (2017). The global distribution of tetrapods
667 reveals a need for targeted reptile conservation. Nat. Ecol. Evol. *1*, 1677–1682.
668 https://doi.org/10.1038/s41559-017-0332-2.

669 36. Cai, L., Kreft, H., Taylor, A., Denelle, P., Schrader, J., Essl, F., van Kleunen, M., Pergl, J.,
670 Pyšek, P., Stein, A., et al. (2023). Global models and predictions of plant diversity based on
671 advanced machine learning techniques. New Phytol. *237*, 1432–1445.
672 https://doi.org/10.1111/nph.18533.

673 37. Ellis, E.C., Antill, E.C., and Kreft, H. (2012). All Is Not Loss: Plant Biodiversity in the
674 Anthropocene. PLOS ONE *7*, e30535. https://doi.org/10.1371/journal.pone.0030535.

675 38. Kreft, H., and Jetz, W. (2007). Global patterns and determinants of vascular plant diversity.
676 Proc. Natl. Acad. Sci. *104*, 5925–5930. https://doi.org/10.1073/pnas.0608361104.

677 39. Fritz, S.A., and Rahbek, C. (2012). Global patterns of amphibian phylogenetic diversity. J.
678 Biogeogr. *39*, 1373–1382. https://doi.org/10.1111/j.1365-2699.2012.02757.x.

679 40. Wolf, S., Mahecha, M.D., Sabatini, F.M., Wirth, C., Bruelheide, H., Kattge, J., Moreno
680 Martínez, Á., Mora, K., and Kattenborn, T. (2022). Citizen science plant observations encode
681 global trait patterns. Nat. Ecol. Evol. *6*, 1850–1859. https://doi.org/10.1038/s41559-022-
682 01904-x.

683 41. Rodrigues, A.S.L., Pilgrim, J.D., Lamoreux, J.F., Hoffmann, M., and Brooks, T.M. (2006).
684 The value of the IUCN Red List for conservation. Trends Ecol. Evol. *21*, 71–76.
685 https://doi.org/10.1016/j.tree.2005.10.010.

686 42. Howard, C., Flather, C.H., and Stephens, P.A. (2020). A global assessment of the drivers of
687 threatened terrestrial species richness. Nat. Commun. *11*, 993. https://doi.org/10.1038/s41467-
688 020-14771-6.

689 43. Hughes, A.C., Orr, M.C., Yang, Q., and Qiao, H. (2021). Effectively and accurately mapping
690 global biodiversity patterns for different regions and taxa. Glob. Ecol. Biogeogr. *30*, 1375–
691 1388. https://doi.org/10.1111/geb.13304.

692 44. Jung, M., Arnell, A., de Lamo, X., García-Rangel, S., Lewis, M., Mark, J., Merow, C., Miles,
693 L., Ondo, I., Pironon, S., et al. (2021). Areas of global importance for conserving terrestrial

biodiversity, carbon and water. Nat. Ecol. Evol. *5*, 1499–1509. https://doi.org/10.1038/s41559-021-01528-7.

45. Mueller, G.M., Cunha, K.M., May, T.W., Allen, J.L., Westrip, J.R.S., Canteiro, C., Costa-Rezende, D.H., Drechsler-Santos, E.R., Vasco-Palacios, A.M., Ainsworth, A.M., et al. (2022). What Do the First 597 Global Fungal Red List Assessments Tell Us about the Threat Status of Fungi? Diversity *14*, 736. https://doi.org/10.3390/d14090736.

46. Locey, K.J., and Lennon, J.T. (2016). Scaling laws predict global microbial diversity. Proc. Natl. Acad. Sci. *113*, 5970–5975. https://doi.org/10.1073/pnas.1521291113.

47. Larsen, B.B., Miller, E.C., Rhodes, M.K., and Wiens, J.J. (2017). Inordinate Fondness Multiplied and Redistributed: the Number of Species on Earth and the New Pie of Life. Q. Rev. Biol. *92*, 229–265. https://doi.org/10.1086/693564.

48. Ruppert, K.M., Kline, R.J., and Rahman, M.S. (2019). Past, present, and future perspectives of environmental DNA (eDNA) metabarcoding: A systematic review in methods, monitoring, and applications of global eDNA. Glob. Ecol. Conserv. *17*, e00547. https://doi.org/10.1016/j.gecco.2019.e00547.

49. Větrovský, T., Morais, D., Kohout, P., Lepinay, C., Algora, C., Awokunle Hollá, S., Bahnmann, B.D., Bílohnědá, K., Brabcová, V., D'Alò, F., et al. (2020). GlobalFungi, a global database of fungal occurrences from high-throughput-sequencing metabarcoding studies. Sci. Data *7*, 228. https://doi.org/10.1038/s41597-020-0567-7.

50. Mikryukov, V., Dulya, O., Zizka, A., Bahram, M., Hagh-Doust, N., Anslan, S., Prylutskyi, O., Delgado-Baquerizo, M., Maestre, F.T., Nilsson, H., et al. (2023). Connecting the multiple dimensions of global soil fungal diversity. Sci. Adv. *9*, eadj8016. https://doi.org/10.1126/sciadv.adj8016.

51. Li, P., Tedersoo, L., Crowther, T.W., Wang, B., Shi, Y., Kuang, L., Li, T., Wu, M., Liu, M., Luan, L., et al. (2023). Global diversity and biogeography of potential phytopathogenic fungi in a changing world. Nat. Commun. *14*, 6482. https://doi.org/10.1038/s41467-023-42142-4.

52. Delgado-Baquerizo, M., Oliverio, A.M., Brewer, T.E., Benavent-González, A., Eldridge, D.J., Bardgett, R.D., Maestre, F.T., Singh, B.K., and Fierer, N. (2018). A global atlas of the dominant bacteria found in soil. Science *359*, 320–325. https://doi.org/10.1126/science.aap9516.

53. Sanderson, E.W., Jaiteh, M., Levy, M.A., Redford, K.H., Wannebo, A.V., and Woolmer, G. (2002). The Human Footprint and the Last of the Wild. BioScience *52*, 891. https://doi.org/10.1641/0006-3568(2002)052[0891:THFATL]2.0.CO;2.

54. Venter, O., Sanderson, E.W., Magrach, A., Allan, J.R., Beher, J., Jones, K.R., Possingham, H.P., Laurance, W.F., Wood, P., Fekete, B.M., et al. (2016). Global terrestrial Human Footprint maps for 1993 and 2009. Sci. Data *3*, 160067. https://doi.org/10.1038/sdata.2016.67.

730 55. Kennedy, C.M., Oakleaf, J.R., Theobald, D.M., Baruch-Mordo, S., and Kiesecker, J. (2019).
731 Managing the middle: A shift in conservation priorities based on the global human
732 modification gradient. Glob. Change Biol. *25*, 811–826. https://doi.org/10.1111/gcb.14549.

733 56. Theobald, D.M., Kennedy, C., Chen, B., Oakleaf, J., Baruch-Mordo, S., and Kiesecker, J.
734 (2020). Earth transformed: detailed mapping of global human modification from 1990 to 2017.
735 Earth Syst. Sci. Data *12*, 1953–1972. https://doi.org/10.5194/essd-12-1953-2020.

736 57. Jung, M., Dahal, P.R., Butchart, S.H.M., Donald, P.F., De Lamo, X., Lesiv, M., Kapos, V.,
737 Rondinini, C., and Visconti, P. (2020). A global map of terrestrial habitat types. Sci. Data *7*,
738 256. https://doi.org/10.1038/s41597-020-00599-8.

739 58. Hansen, M.C., Potapov, P.V., Moore, R., Hancher, M., Turubanova, S.A., Tyukavina, A.,
740 Thau, D., Stehman, S.V., Goetz, S.J., Loveland, T.R., et al. (2013). High-Resolution Global
741 Maps of 21st-Century Forest Cover Change. Science *342*, 850–853.
742 https://doi.org/10.1126/science.1244693.

743 59. Lang, N., Jetz, W., Schindler, K., and Wegner, J.D. (2023). A high-resolution canopy height
744 model of the Earth. Nat. Ecol. Evol. *7*, 1778–1789. https://doi.org/10.1038/s41559-023-
745 02206-6.

746 60. Spawn, S.A., Sullivan, C.C., Lark, T.J., and Gibbs, H.K. (2020). Harmonized global maps of
747 above and belowground biomass carbon density in the year 2010. Sci. Data *7*, 112.
748 https://doi.org/10.1038/s41597-020-0444-4.

749 61. Ma, H., Mo, L., Crowther, T.W., Maynard, D.S., Van Den Hoogen, J., Stocker, B.D., Terrer,
750 C., and Zohner, C.M. (2021). The global distribution and environmental drivers of
751 aboveground versus belowground plant biomass. Nat. Ecol. Evol. *5*, 1110–1122.
752 https://doi.org/10.1038/s41559-021-01485-1.

753 62. Warner, D.L., Bond-Lamberty, B.P., Jian, J., Stell, E., and Vargas, R. (2019). Carbon
754 Monitoring System (CMS)Global Gridded 1-km Annual Soil Respiration and Uncertainty
755 Derived from SRDB V3. Preprint at ORNL Distributed Active Archive Center,
756 https://doi.org/10.3334/ORNLDAAC/1736 https://doi.org/10.3334/ORNLDAAC/1736.

757 63. Tuanmu, M.-N., and Jetz, W. (2015). A global, remote sensing-based characterization of
758 terrestrial habitat heterogeneity for biodiversity and ecosystem modelling. Glob. Ecol.
759 Biogeogr. *24*, 1329–1339. https://doi.org/10.1111/geb.12365.

760 64. Myneni, R., Knyazikhin, Y., and Park, T. (2021). MODIS/Terra+Aqua Leaf Area Index/FPAR
761 4-Day L4 Global 500m SIN Grid V061. (NASA EOSDIS Land Processes Distributed Active
762 Archive Center). https://doi.org/10.5067/MODIS/MCD15A3H.061
763 https://doi.org/10.5067/MODIS/MCD15A3H.061.

764 65. Cisneros-Araujo, P., Goicolea, T., Mateo-Sánchez, M.C., García-Viñás, J.I., Marchamalo, M.,
765 Mercier, A., and Gastón, A. (2021). The Role of Remote Sensing Data in Habitat Suitability

and Connectivity Modeling: Insights from the Cantabrian Brown Bear. Remote Sens. *13*, 1138. https://doi.org/10.3390/rs13061138.

66. Cisneros-Araujo, P., Ramirez-Lopez, M., Juffe-Bignoli, D., Fensholt, R., Muro, J., Mateo-Sánchez, M.C., and Burgess, N.D. (2021). Remote sensing of wildlife connectivity networks and priority locations for conservation in the Southern Agricultural Growth Corridor (SAGCOT) in Tanzania. Remote Sens. Ecol. Conserv. *7*, 430–444. https://doi.org/10.1002/rse2.199.

67. Running, S.W., and Zhao, M. Daily GPP and Annual NPP (MOD17A2/A3) Products NASA Earth Observing System MODIS Land Algorithm.

68. Smith, T., Traxl, D., and Boers, N. (2022). Empirical evidence for recent global shifts in vegetation resilience. Nat. Clim. Change *12*, 477–484. https://doi.org/10.1038/s41558-022-01352-2.

69. Seddon, A.W.R., Macias-Fauria, M., Long, P.R., Benz, D., and Willis, K.J. (2016). Sensitivity of global terrestrial ecosystems to climate variability. Nature *531*, 229–232. https://doi.org/10.1038/nature16986.

70. Giri, C., Ochieng, E., Tieszen, L.L., Zhu, Z., Singh, A., Loveland, T., Masek, J., and Duke, N. (2011). Status and distribution of mangrove forests of the world using earth observation satellite data. Glob. Ecol. Biogeogr. *20*, 154–159. https://doi.org/10.1111/j.1466-8238.2010.00584.x.

71. Xu, J., Morris, P.J., Liu, J., and Holden, J. (2018). PEATMAP: Refining estimates of global peatland distribution based on a meta-analysis. CATENA *160*, 134–140. https://doi.org/10.1016/j.catena.2017.09.010.

72. T., G., R.M., R.-C., L.V., V., M., H., F., W., E., H., N., H., and D., M. Tropical and Subtropical Wetlands Distribution version 2. https://doi.org/10.17528/cifor/data.00058 https://doi.org/10.17528/cifor/data.00058.

73. Mendes, S.B., Olesen, J.M., Memmott, J., Costa, J.M., Timóteo, S., Dengucho, A.L., Craveiro, L., and Heleno, R. (2024). Evidence of a European seed dispersal crisis. Science *386*, 206–211. https://doi.org/10.1126/science.ado1464.

74. GFBI consortium, Steidinger, B.S., Crowther, T.W., Liang, J., Van Nuland, M.E., Werner, G.D.A., Reich, P.B., Nabuurs, G.J., de-Miguel, S., Zhou, M., et al. (2019). Climatic controls of decomposition drive the global biogeography of forest-tree symbioses. Nature *569*, 404–408. https://doi.org/10.1038/s41586-019-1128-0.

75. Barceló, M., Van Bodegom, P.M., and Soudzilovskaia, N.A. (2023). Fine-resolution global maps of root biomass carbon colonized by arbuscular and ectomycorrhizal fungi. Sci. Data *10*, 56. https://doi.org/10.1038/s41597-022-01913-2.

76. Rodell, M., Houser, P.R., Jambor, U., Gottschalck, J., Mitchell, K., Meng, C.-J., Arsenault, K., Cosgrove, B., Radakovich, J., Bosilovich, M., et al. (2004). The Global Land Data Assimilation System. Bull. Am. Meteorol. Soc. *85*, 381–394. https://doi.org/10.1175/BAMS-85-3-381.

77. Tuomi, M., Laiho, R., Repo, A., and Liski, J. (2011). Wood decomposition model for boreal forests. Ecol. Model. *222*, 709–718. https://doi.org/10.1016/j.ecolmodel.2010.10.025.

78. Assis, J.C., Hohlenwerger, C., Metzger, J.P., Rhodes, J.R., Duarte, G.T., da Silva, R.A., Boesing, A.L., Prist, P.R., and Ribeiro, M.C. (2023). Linking landscape structure and ecosystem service flow. Ecosyst. Serv. *62*, 101535. https://doi.org/10.1016/j.ecoser.2023.101535.

79. Baude, M., and Meyer, B.C. (2023). Changes in landscape structure and ecosystem services since 1850 analyzed using landscape metrics in two German municipalities. Ecol. Indic. *152*, 110365. https://doi.org/10.1016/j.ecolind.2023.110365.

80. Belote, R.T., Barnett, K., Zeller, K., Brennan, A., and Gage, J. (2022). Examining local and regional ecological connectivity throughout North America. Landsc. Ecol. *37*, 2977–2990. https://doi.org/10.1007/s10980-022-01530-9.

81. Beyer, H.L., Venter, O., Grantham, H.S., and Watson, J.E.M. (2020). Substantial losses in ecoregion intactness highlight urgency of globally coordinated action. Conserv. Lett. *13*, e12692. https://doi.org/10.1111/conl.12692.

82. Liu, S., Dong, Y., Deng, L., Liu, Q., Zhao, H., and Dong, S. (2014). Forest fragmentation and landscape connectivity change associated with road network extension and city expansion: A case study in the Lancang River Valley. Ecol. Indic. *36*, 160–168. https://doi.org/10.1016/j.ecolind.2013.07.018.

83. Hill, S.L.L., Fajardo, J., Maney, C., Harfoot, M., Harrison, M., Guaras, D., Jones, M., Oliva, M.J., Danks, F., Hughes, J., et al. (2022). The Ecosystem Integrity Index: a novel measure of terrestrial ecosystem integrity with global coverage (Ecology) https://doi.org/10.1101/2022.08.21.504707.

84. Newbold, T., Hudson, L.N., Arnell, A.P., Contu, S., De Palma, A., Ferrier, S., Hill, S.L.L., Hoskins, A.J., Lysenko, I., Phillips, H.R.P., et al. (2016). Has land use pushed terrestrial biodiversity beyond the planetary boundary? A global assessment. Science *353*, 288–291. https://doi.org/10.1126/science.aaf2201.

85. De Palma, A., Hoskins, A., Gonzalez, R.E., Börger, L., Newbold, T., Sanchez-Ortiz, K., Ferrier, S., and Purvis, A. (2021). Annual changes in the Biodiversity Intactness Index in tropical and subtropical forest biomes, 2001–2012. Sci. Rep. *11*, 20249. https://doi.org/10.1038/s41598-021-98811-1.

86. Schipper, A.M., Hilbers, J.P., Meijer, J.R., Antão, L.H., Benítez-López, A., de Jonge, M.M.J., Leemans, L.H., Scheper, E., Alkemade, R., Doelman, J.C., et al. (2020). Projecting terrestrial biodiversity intactness with GLOBIO 4. Glob. Change Biol. *26*, 760–771. https://doi.org/10.1111/gcb.14848.

87. Hill, S.L.L., Gonzalez, R., Sanchez-Ortiz, K., Caton, E., Espinoza, F., Newbold, T., Tylianakis, J., Scharlemann, J.P.W., De Palma, A., and Purvis, A. (2018). Worldwide impacts of past and projected future land-use change on local species richness and the Biodiversity Intactness Index (Ecology) https://doi.org/10.1101/311787.

88. Hudson, L.N., Newbold, T., Contu, S., Hill, S.L.L., Lysenko, I., De Palma, A., Phillips, H.R.P., Senior, R.A., Bennett, D.J., Booth, H., et al. (2014). The PREDICTS database: a global database of how local terrestrial biodiversity responds to human impacts. Ecol. Evol. *4*, 4701–4735. https://doi.org/10.1002/ece3.1303.

89. Hudson, L.N., Newbold, T., Contu, S., Hill, S.L.L., Lysenko, I., De Palma, A., Phillips, H.R.P., Alhusseini, T.I., Bedford, F.E., Bennett, D.J., et al. (2017). The database of the PREDICTS (Projecting Responses of Ecological Diversity In Changing Terrestrial Systems) project. Ecol. Evol. *7*, 145–188. https://doi.org/10.1002/ece3.2579.

90. Liu, L., Zhu, K., Wurzburger, N., and Zhang, J. (2020). Relationships between plant diversity and soil microbial diversity vary across taxonomic groups and spatial scales. Ecosphere *11*, e02999. https://doi.org/10.1002/ecs2.2999.

91. Prober, S.M., Leff, J.W., Bates, S.T., Borer, E.T., Firn, J., Harpole, W.S., Lind, E.M., Seabloom, E.W., Adler, P.B., Bakker, J.D., et al. (2015). Plant diversity predicts beta but not alpha diversity of soil microbes across grasslands worldwide. Ecol. Lett. *18*, 85–95. https://doi.org/10.1111/ele.12381.

92. Kwok, R. (2018). Ecology's remote-sensing revolution. Nature *556*, 137–138. https://doi.org/10.1038/d41586-018-03924-9.

93. Farley, S.S., Dawson, A., Goring, S.J., and Williams, J.W. (2018). Situating Ecology as a Big-Data Science: Current Advances, Challenges, and Solutions. BioScience *68*, 563–576. https://doi.org/10.1093/biosci/biy068.

94. Abe, S. (2005). Training of Support Vector Machines with Mahalanobis Kernels. In Artificial Neural Networks: Formal Models and Their Applications – ICANN 2005 Lecture Notes in Computer Science., W. Duch, J. Kacprzyk, E. Oja, and S. Zadrożny, eds. (Springer Berlin Heidelberg), pp. 571–576. https://doi.org/10.1007/11550907_90.

95. Dinerstein, E., Olson, D., Joshi, A., Vynne, C., Burgess, N.D., Wikramanayake, E., Hahn, N., Palminteri, S., Hedao, P., Noss, R., et al. (2017). An Ecoregion-Based Approach to Protecting Half the Terrestrial Realm. BioScience *67*, 534–545. https://doi.org/10.1093/biosci/bix014.

96. Suding, K.N. (2011). Toward an Era of Restoration in Ecology: Successes, Failures, and Opportunities Ahead. Annu. Rev. Ecol. Evol. Syst. *42*, 465–487. https://doi.org/10.1146/annurev-ecolsys-102710-145115.

97. Balaguer, L., Escudero, A., Martín-Duque, J.F., Mola, I., and Aronson, J. (2014). The historical reference in restoration ecology: Re-defining a cornerstone concept. Biol. Conserv. *176*, 12–20. https://doi.org/10.1016/j.biocon.2014.05.007.

98. Runfola, D., Anderson, A., Baier, H., Crittenden, M., Dowker, E., Fuhrig, S., Goodman, S., Grimsley, G., Layko, R., Melville, G., et al. (2020). geoBoundaries: A global database of political administrative boundaries. PLOS ONE *15*, e0231866. https://doi.org/10.1371/journal.pone.0231866.

99. Jetz, W., McPherson, J.M., and Guralnick, R.P. (2012). Integrating biodiversity distribution knowledge: toward a global map of life. Trends Ecol. Evol. *27*, 151–159. https://doi.org/10.1016/j.tree.2011.09.007.

100. Paz, A., Silva, T.S., and Carnaval, A.C. (2022). A framework for near-real time monitoring of diversity patterns based on indirect remote sensing, with an application in the Brazilian Atlantic rainforest. PeerJ *10*, e13534. https://doi.org/10.7717/peerj.13534.

101. Turner, W. (2014). Sensing biodiversity. Science *346*, 301–302. https://doi.org/10.1126/science.1256014.

102. Cawse-Nicholson, K., Townsend, P.A., Schimel, D., Assiri, A.M., Blake, P.L., Buongiorno, M.F., Campbell, P., Carmon, N., Casey, K.A., Correa-Pabón, R.E., et al. (2021). NASA's surface biology and geology designated observable: A perspective on surface imaging algorithms. Remote Sens. Environ. *257*, 112349. https://doi.org/10.1016/j.rse.2021.112349.

103. European Space Agency (2020). Chime (Copernicus Hyperspectral Imaging Mission for the Environment) - eoPortal. https://www.eoportal.org/satellite-missions/chime-copernicus#eop-quick-facts-section.

104. Cavender-Bares, J., Gamon, J.A., Hobbie, S.E., Madritch, M.D., Meireles, J.E., Schweiger, A.K., and Townsend, P.A. (2017). Harnessing plant spectra to integrate the biodiversity sciences across biological and spatial scales. Am. J. Bot. *104*, 966–969. https://doi.org/10.3732/ajb.1700061.

105. Deiner, K., Bik, H.M., Mächler, E., Seymour, M., Lacoursière-Roussel, A., Altermatt, F., Creer, S., Bista, I., Lodge, D.M., de Vere, N., et al. (2017). Environmental DNA metabarcoding: Transforming how we survey animal and plant communities. Mol. Ecol. *26*, 5872–5895. https://doi.org/10.1111/mec.14350.

106. Sueur, J., and Farina, A. (2015). Ecoacoustics: the Ecological Investigation and Interpretation of Environmental Sound. Biosemiotics *8*, 493–502. https://doi.org/10.1007/s12304-015-9248-x.

907 107. Buřivalová, Z., Yoh, N., Butler, R.A., Chandra Sagar, H.S.S., and Game, E.T. (2023).
908 Broadening the focus of forest conservation beyond carbon. Curr. Biol. *33*, R621–R635.
909 https://doi.org/10.1016/j.cub.2023.04.019.

910 108. Dasgupta, P. (2021). The Economics of Biodiversity: The Dasgupta Review.

911 109. The Bonn Challenge | Bonchallenge https://www.bonnchallenge.org/.

912 110. THE 17 GOALS | Sustainable Development https://sdgs.un.org/goals.

913 111. Science Based Targets Network Sci. Based Targets Netw.
914 https://sciencebasedtargetsnetwork.org/.

915 112. European Space Agency (2022). Copernicus Sentinel-2 (processed by ESA), 2022, MSI
916 Level-2A BOA Reflectance Product. Collection 1.

917 113. Sabatini, F.M., Jiménez-Alfaro, B., Jandt, U., Chytrý, M., Field, R., Kessler, M., Lenoir, J.,
918 Schrodt, F., Wiser, S.K., Arfin Khan, M.A.S., et al. (2022). Global patterns of vascular plant
919 alpha diversity. Nat. Commun. *13*, 4683. https://doi.org/10.1038/s41467-022-32063-z.

920 114. Sanchez-Ortiz, K., Gonzalez, R.E., De Palma, A., Newbold, T., Hill, S.L.L., Tylianakis, J.M.,
921 Börger, L., Lysenko, I., and Purvis, A. (2019). Land-use and related pressures have reduced
922 biotic integrity more on islands than on mainlands. Preprint, https://doi.org/10.1101/576546
923 https://doi.org/10.1101/576546.

924 115. Impact Observatory and Vizzuality Biodiversity Intactness Index (BII). (Google Earth
925 Engine:projects/ebx-data/assets/earthblox/IO/BIOINTACT).

926

Supplement S1. Materials and methods

1. Reference Area Methodology

We developed an approach that offers a contemporary baseline in which all global biodiversity maps may be evaluated. Our algorithm uses the human modification index (HMI)[55] and potential natural vegetation (PNV)[57] to create a reference area mask that delineates the relatively pristine areas on the globe. The combination of PNV classes and 846 delineated ecoregions[95] then guides the assignment of reference areas to all non-reference pixels having the same ecoregion-PNV class. Due to the large variations in the extent of human modification among different ecoregion landcover combinations, we designed a dynamic decision tree for selecting a threshold HMI to define reference pixels and then to link reference to non-reference pixels to obtain the reference mask.

We targeted reference pixels with minimal human modification which we defined as follows. For each PNV class, v, within each ecoregion, e, we calculated the 5th and 3rd percentile of the HMI, $P_{0.05}(HMI_{e,v})$ and $P_{0.03}(HMI_{e,v})$. The reference threshold value, $r_{e,v}$ was then set to the maximum of either $P_{0.05}(HMI_{e,v})$ or $P_{0.03}(HMI_{e,v})$ if they were less than 0.05, or 0.05 (See equation S1 below).

$$r_{e,v} = \begin{cases} P_{0.05}(HMI_{e,v}) & if\ P_{0.05}(HMI_{e,v}) \leq 0.05 \\ P_{0.03}(HMI_{e,v}) & if\ P_{0.05}(HMI_{e,v}) > 0.05\ and\ P_{0.03}(HMI_{e,v}) \leq 0.05 \\ 0.05 & if\ P_{0.05}(HMI_{e,v}) > 0.05\ and\ P_{0.03}(HMI_{e,v}) > 0.05 \end{cases} \quad \text{Equation S1}$$

Within relatively unmodified ecoregions, we set more restrictive criteria to refine and focus the selected reference areas to include only pixels with very low HMI. In more thoroughly modified ecoregions, we loosened the criteria for more inclusion in selected reference areas, but only to the point of an HMI equal to 0.05. With the threshold defined for each ecoregion-PNV class, we selected reference areas as all pixels less than $r_{e,v}$. If an ecoregion-PNV class had fewer than five pixels, we stepped down the reference threshold – from the $P_{0.05}(HMI_{e,v})$ to $P_{0.03}(HMI_{e,v})$, or from $P_{0.03}(HMI_{e,v})$ to $0.05(x_{e,v}, y_{e,v})$. If $r_{e,v}$ was 0.05, and the ecoregion-PNV class still possessed fewer than five reference pixels, then we looked beyond the ecoregion boundary and included all reference pixels of the same PNV class within the same biome.

2. Delta calculation

To calculate the delta value for each axis (subindex) of the seed index, we use the following formula:

$$K = e^{-\delta D}$$

where K is the kernel, δ is the delta parameter and D is the maximum Manhattan distance of the axis for all the pixel points. δmediates the translation of distance to similarity, effectively maping the highest possible distance to the lowest kernel value (K > 0). Tuning δ shifts the balance between similarity and dissimilarity. Balance in our case was achieved by equating the highest distance to the lowest similarity, a kernel value of 0.001, and solving for the δ value for each of the axis. We then substitute this delta value in the equation to calculate the kernel for the world of each axis. The SEED index is then calculated based on the weighted average of the individual axes.

3. Weighting system

We considered two points of information in calculating the normalized weight for each map layer: the hierarchical structuring of data layers into groups and our confidence in each individual layer. Similar types of data were paired evenly at each level of the hierarchy (Figure S1) to ensure both averaging of duplicate information and equal weighting among components at the same level.

We ranked our confidence in each map layer based on several features: underlying predictive layers, quality of validation data (including spatial coverage), spatial resolution, and perceived error at SEED's 1-km resolution. We defined five rank classes associated with percent scores (Table S1). The scores associated with each ranking are tunable parameters. We opted for skewed mid-level scores, with medium high scoring 90% and medium low scoring 10%.

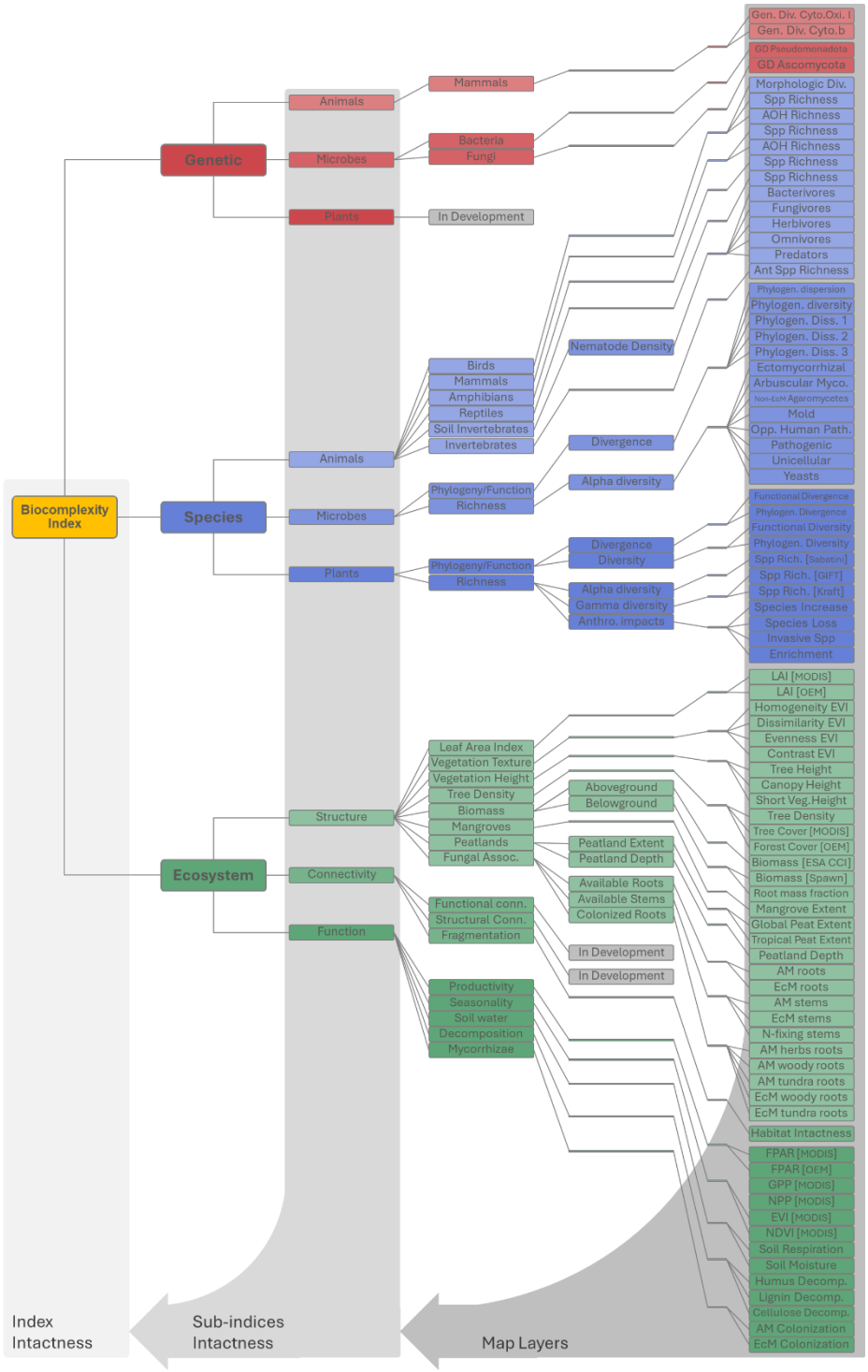

Figure S1. Hierarchy of information. Hierarchy of global biodiversity map layers (branch tips) that feed into the nine sub-indices (Figure 2) and then into the headline biocomplexity index. Details for each map are listed in supplemental Table S2.

979 **Table S1.** Table of scores, weights, and a description of the criteria guiding our judgment in rating
980 the quality of information contained with each map that we incorporated in SEED.

Confidence Score	Weight	Description
5	100	Fully validated model representing on the ground conditions with at least 1-km resolution
4	90	Partially validated model representing on the ground conditions with at least 1-km resolution
3	50	Model predicting on the ground conditions with at least 5-km resolution, requires validation
2	10	Model predicting general diversity patterns with some human impacts considered
1	1	Model of general diversity patterns. Does not represent human impacts on nature.

981

Table S2. List of global biodiversity maps alongside their unique details (resolution, units, and citations) our confidence scores and the normalized weights. For interactive links see online table

Index	Weight	Axis	Branch 1	Branch 2	Layer Name	Conf. Score	Weight	Data Name / Description	Original Spatial Resolution	Units	Source	Citation
Biocomplexity	0.09242	ecosystem_connectivity	ec_fragmentation		habitat_intactness	50	0.0924	Habitat integrity, measured by Human Footprint	≈11 km	proportion (0-1)	Methodolgy from (Beyer et al. 2019)	https://doi.org/10.1111/conl.12692
	0.18484	ecosystem_function	ef_productivity		modis_fpar	100	0.0227	Fraction of incident photosynthetically active radiation (400-700nm) absorbed by the green elements of a vegetation canopy	≈500 m	Fpar fraction	https://explorer.earthengine.google.com/#detail/MODIS%2F006%2FMCD15A3H	https://doi.org/10.5067/MODIS/MCD15A3H.006
					oem_fpar	100	0.0227	Fraction of incident photosynthetically active radiation (400-700nm) absorbed by the green elements of a vegetation canopy	≈10 m	Fpar fraction	In Review	In Review
					modis_gpp	100	0.0227	MOD17A3.055: Terra Gross Primary Production Yearly Global 1km	≈1 km	0.0001 * kg*C/m^2	https://explorer.earthengine.google.com/#detail/MODIS%2F055%2FMOD17A3	https://lpdaac.usgs.gov/products/mod17a3v055/
					modis_npp	100	0.0227	MOD17A3.055: Terra Net Primary Production Yearly Global 1km	≈1 km	0.0001 * kg*C/m^2	https://explorer.earthengine.google.com/#detail/MODIS%2F055%2FMOD17A3	https://lpdaac.usgs.gov/products/mod17a3v055/
			ef_seasonality		modis_evi	100	0.0453	MYD13Q1.006 Vegetation Indices 16-Day Global 250m: NDVI and EVI	≈250 m	EVI Value	https://explorer.earthengine.google.com/#detail/MODIS%2F006%2FMYD13Q1	https://doi.org/10.5067/MODIS/MYD13Q1.006
					modis_ndvi	100	0.0453	MYD13Q1.006 Vegetation Indices 16-Day Global 250m: NDVI and EVI	≈250 m	NDVI Value	https://explorer.earthengine.google.com/#detail/MODIS%2F006%2FMYD13Q1	https://doi.org/10.5067/MODIS/MYD13Q1.006
			ef_respiration		soil_respiration	1	0.0009	Mean annual rate of soil respiration	≈900 m	g C / m^2 * y	https://daac.ornl.gov/CMS/guides/CMS_Global_Soil_Respiration.html	https://doi.org/10.3334/ORNLDAAC/1736
			ef_soil_water		soil_moisture	1	0.0009	Mean annual soil moisture	≈11 km	kg/m2	https://code.earthengine.google.com/d704d1a6f45a6b717eb83640ef200227	https://doi.org/10.1175/BAMS-85-3-381;
			ef_decomp		decomp_humus	1	0.0003	Decomposition coefficients for humus based on the Yasso15 model.	≈900 m	Unitless	https://en.ilmatieteenlaitos.fi/yasso-description	https://doi.org/10.1016/j.ecolmodel.2010.10.025
					decomp_lignin	1	0.0003	Decomposition coefficients for lignin based on the Yasso15 model.	≈900 m	Unitless	https://en.ilmatieteenlaitos.fi/yasso-description	https://doi.org/10.1016/j.ecolmodel.2010.10.025
					decomp_cellulose	1	0.0003	Decomposition coefficients for sugars, cellulose and wax-like compounds based on the Yasso15 model.	≈900 m	Unitless	https://en.ilmatieteenlaitos.fi/yasso-description	https://doi.org/10.1016/j.ecolmodel.2010.10.025
			ef_myco_colonization		AM_intensity_colonization	1	0.0005	The intensity of AM root colonization	≈18 km	%	https://www.nature.com/articles/s41597-022-01913-2	https://www.nature.com/articles/s41597-022-01913-2
					EcM_intensity_colonization	1	0.0005	The intensity of EcM root colonization	≈18 km	%	https://www.nature.com/articles/s41597-022-01913-2	https://www.nature.com/articles/s41597-022-01913-2
	0.18484	ecosystem_structure	es_leaf_area_index		lai	100	0.0130	Leaf Area Index (LAI) = MCD15A3H.006 Terra+Aqua Leaf Area Index	≈500 m	LAI value	https://explorer.earthengine.google.com/#detail/MODIS%2F006%2FMCD15A3H	https://doi.org/10.5067/MODIS/MCD15A3H.006
					oem_lai	100	0.0130	Leaf Area Index (LAI)	≈10 m	LAI value	In Review	In Review
			es_foliage_homogen		evi_homogeneity	100	0.0065	Homogeneity (EVI Heterogeneity); Similarity of EVI between adjacent pixels	≈1 km	>=0; <=1	http://www.earthenv.org/texture	https://doi.org/10.1111/geb.12365
					evi_dissimilarity	100	0.0065	Dissimilarity (EVI Heterogeneity); Difference in EVI between adjacent pixels	≈1 km	>=0	http://www.earthenv.org/texture	https://doi.org/10.1111/geb.12365
					evi_evenness	100	0.0065	Evenness (EVI Heterogeneity); Evenness of EVI	≈1 km	>=0; <=1	http://www.earthenv.org/texture	https://doi.org/10.1111/geb.12365
					evi_contrast	100	0.0065	Contrast (EVI Heterogeneity); Exponentially weighted difference in EVI between adjacent pixels	≈1 km	>=0	http://www.earthenv.org/texture	https://doi.org/10.1111/geb.12365
			es_veg_height		treeheight	100	0.0087	Global Canopy Height 2020	≈30 m	height in meters	https://glad.geog.umd.edu/dataset/GLCLUC2020	https://doi.org/10.3389/frsen.2022.856903
					canheight	100	0.0087	ETH Global Canopy Height 2020	≈10 m	height in meters	https://doi.org/10.3929/ethz-b-000609802	https://doi.org/10.1038/s41559-023-02206-6
					shveg_height	100	0.0087	Short vegetation height	≈30 m	height in meters	https://doi.org/10.5281/zenodo.15198675	https://doi.org/10.1038/s41597-024-04139-6
			es_tree_density		tree_density	90	0.0081	Tree (Stem) Density	≈1 km	no of stems per pixel	http://elischolar.library.yale.edu/yale_fes_data/1/	https://doi.org/10.1038/nature14967
					treecov	100	0.0090	Tree canopy cover for year 2020, defined as canopy closure for all vegetation taller than 5m in height. (Hansen et al.)	≈30 m	Canopy closure (0-100%)	https://glad.umd.edu/dataset/global-2010-tree-cover-30-m	https://doi.org/10.1126/science.1244693
					oem_fcover	100	0.0090	Forest cover for 2024 created by Felix Specker for Open Earth Monitor	≈100 m	>=0; <=1	In Review	In Review
			es_plant_biomass	es_aboveground_biom	esa_cci_agb	100	0.0137	ESA CCI Above ground biomass for the year 2022	≈100 m	Mg C / ha	https://data.ceda.ac.uk/neodc/esacci/biomass/data/agb/maps/v2.0/geotiff	http://dx.doi.org/10.5285/84403d09cef3485883158f4df2989b0c
				es_belowground_biom	bgb_spawn	90	0.0062	Global belowground biomass carbon density for the year 2010 (Spawn et al)	≈300 m	Mg C / ha	https://doi.org/10.3334/ORNLDAAC/1763	https://doi.org/10.1038/s41597-020-0444-4
					root_mass_fraction	90	0.0062	Root mass fraction describes the plant biomass distributions below- versus aboveground (Ma et al)	≈30 m	%	https://doi.org/10.1038/s41559-021-01485-1	https://doi.org/10.1038/s41559-021-01485-1
			es_mangrove_extent		mangroves_girietal	100	0.0260	Mangroves extent for the year 2000 (Giri et al)	≈30 m	Unitless	https://developers.google.com/earth-engine/datasets/catalog/LANDSAT_MANGROVE_FO	https://doi.org/10.7927/H4J67DW8; https://doi.org/10.1111/j.1466-
			es_peatlands	es_peat_extent	global_peatland_extent	100	0.0065	Global Peatland distribution. This layer was created from the PEATMAP polygons.	≈230 m	%	http://archive.researchdata.leeds.ac.uk/251/	https://doi.org/10.1016/j.catena.2017.09.010
					tropical_peatland_extent	100	0.0065	Tropical and subtropical peatland extent (CIFOR)	≈230 m	Unitless	https://onlinelibrary.wiley.com/doi/full/10.1111/gcb.13689	https://doi.org/10.17528/CIFOR/DATA.00058
				es_peat_depth	tropical_peatland_depth	100	0.0130	Tropical and subtropical peatland depth (CIFOR)	≈230 m	depth in meters	https://onlinelibrary.wiley.com/doi/full/10.1111/gcb.13689	https://doi.org/10.17528/CIFOR/DATA.00058
			es_fungal_assoc	es_avail_fine_roots	AM_roots	10	0.0004	Fine root biomass C stocks that are capable to form associations with AM fungi	≈18 km	Mg C / ha	https://doi.org/10.5061/dryad.866t1g1tt	https://www.nature.com/articles/s41597-022-01913-2
					EcM_roots	10	0.0004	Fine root biomass C stocks that are capable to form associations with EcM fungi	≈18 km	Mg C / ha	https://doi.org/10.5061/dryad.866t1g1tt	https://www.nature.com/articles/s41597-022-01913-2
				es_avail_stems	AM_stems	10	0.0003	Estimated proportion of arbuscular mycorrhizal related woody stems (above 10cm). (downsampled100km)	≈111 km	proportion (0-1)	https://www.nature.com/articles/s41586-019-1128-0	https://www.nature.com/articles/s41586-019-1128-0
					EM_stems	10	0.0003	Estimated proportion of ecto-mycorrhizal related woody stems (above 10cm). (downsampled100km)	≈111 km	proportion (0-1)	https://www.nature.com/articles/s41586-019-1128-0	https://www.nature.com/articles/s41586-019-1128-0
					Nfix_stems	10	0.0003	Estimated proportion of nitrogen-fixing mycorrhizal related woody stems (above 10cm). (downsampled100km)	≈111 km	proportion (0-1)	https://www.nature.com/articles/s41586-019-1128-0	https://www.nature.com/articles/s41586-019-1128-0
				es_colonized_fine_roots	AM_herbs_roots_colonized	10	0.0002	Herbaceous fine root biomass carbon stocks associated with AM fungi	≈18 km	Mg C / ha	https://doi.org/10.5061/dryad.866t1g1tt	https://www.nature.com/articles/s41597-022-01913-2
					AM_woody_roots_colonized	10	0.0002	Woody fine root biomass carbon stocks associated with AM fungi	≈18 km	Mg C / ha	https://doi.org/10.5061/dryad.866t1g1tt	https://www.nature.com/articles/s41597-022-01913-2
					AM_tundra_roots_colonized	10	0.0002	Tundra fine root biomass carbon stocks associated with AM fungi	≈18 km	Mg C / ha	https://doi.org/10.5061/dryad.866t1g1tt	https://www.nature.com/articles/s41597-022-01913-2
					EcM_woody_roots_colonized	10	0.0002	Woody fine root biomass carbon stocks associated with EcM fungi	≈18 km	Mg C / ha	https://doi.org/10.5061/dryad.866t1g1tt	https://www.nature.com/articles/s41597-022-01913-2
					EcM_tundra_roots_colonized	10	0.0002	Tundra fine root biomass carbon stocks associated with EcM fungi	≈18 km	Mg C / ha	https://doi.org/10.5061/dryad.866t1g1tt	https://www.nature.com/articles/s41597-022-01913-2
	0.01848	genetic_animals	ga_mitoch_diversity		ga_mammals_c01	10	0.0092	Genetic diversity of Cytochrome b	≈386 km	proportion (0-1)	https://github.com/spyrostheodoridis/Genetic-geography-of-terrestrial-mammals	https://www.nature.com/articles/s41467-020-16449-5
					ga_mammals_cytb	10	0.0092	Genetic diversity of Cytochrome oxidase I	≈386 km	proportion (0-1)	https://github.com/spyrostheodoridis/Genetic-geography-of-terrestrial-mammals	https://www.nature.com/articles/s41467-020-16449-5
	0.09242	genetic_microbes	gm_bacteria		gm_pseudomonadota	50	0.0462	Nucleotide diversity (the average proportion of nucleotide differences between any two randomly selected DNA sequences)	≈1 km	proportion (0-1)	https://zenodo.org/records/16534882	https://doi.org/10.5281/zenodo.16534881
			gm_fungi		gm_ascomycota	50	0.0462	Nucleotide diversity (the average proportion of nucleotide differences between any two randomly selected DNA sequences)	≈1 km	proportion (0-1)	https://zenodo.org/records/16534882	https://doi.org/10.5281/zenodo.16534881
	0.00185	genetic_plants	gp_dummy		dummy_gp	1	0.0018	Placeholder blank layer	≈1 km	proportion (0-1)	Blank map with 1.0 values everywhere	NA
	0.16636	species_animals	sa_avian_diveristy		birds_morpho	1	0.0006	Hughes et al. Global biogeographic patterns of avian morphological diversity. Ecology Letters.	≈100 km	Morphological variance (sum of	https://doi.org/10.15131/shef.data.16733224.v2	https://doi.org/10.1111/ele.13905
					birds_richness	10	0.0059	Jenkins2013_BirdsRichness	≈10 km	No. spp (gamma diversity)	BirdLife Int	https://www.pnas.org/doi/abs/10.1073/pnas.1302251110
					bird_aoh_richness	90	0.0532	Area of Habitat maps for the world's terrestrial birds	≈100 m	No. spp	https://doi.org/10.5061/dryad.02v6wwq48	https://doi.org/10.5194/gmd-15-5093-2022
			sa_mammal_diversity		mammals_richness	10	0.0060	Jenkins2013_MammalsRichness	≈10 km	No. spp (gamma diversity)	IUCN	https://www.pnas.org/doi/abs/10.1073/pnas.1302251110
					mammal_aoh_richness	90	0.0537	Area of Habitat maps for the world's terrestrial mammals	≈100 m	No. spp	https://doi.org/10.5061/dryad.02v6wwq48	https://doi.org/10.5194/gmd-15-5093-2022
			sa_amphib_diversity		amphibians_richness	50	0.0331	Jenkins2013_AmphibiansRichness	≈10 km	No. spp (gamma diversity)	IUCN	https://www.pnas.org/doi/abs/10.1073/pnas.1302251110
			sa_reptile_diversity		reptile_richness	10	0.0066	The global distribution of tetrapods reveals a need for targeted reptile conservation (Roll et al)	≈48 km	No. spp	https://doi.org/10.5061/dryad.83s7k	https://www.nature.com/articles/s41559-017-0332-2
			sa_soil_invertebrates		nematodes_bacterivores	10	0.0013	Number of Bacterivore Nematodes estimated per 100g of soil	≈900 m	# of expected nematodes	https://doi.org/10.3929/ethz-b-000354394	https://www.nature.com/articles/s41586-019-1418-6
					nematodes_fungivores	10	0.0013	Number of Fungivore Nematodes estimated per 100g of soil	≈900 m	# of expected nematodes	https://doi.org/10.3929/ethz-b-000354394	https://www.nature.com/articles/s41586-019-1418-6
					nematodes_herbivores	10	0.0013	Number of Herbivores Nematodes estimated per 100g of soil	≈900 m	# of expected nematodes	https://doi.org/10.3929/ethz-b-000354394	https://www.nature.com/articles/s41586-019-1418-6
					nematodes_omnivore	10	0.0013	Number of Omnivore Nematodes estimated per 100g of soil	≈900 m	# of expected nematodes	https://doi.org/10.3929/ethz-b-000354394	https://www.nature.com/articles/s41586-019-1418-6
					nematodes_predators	10	0.0013	Number of Predator Nematodes estimated per 100g of soil	≈900 m	# of expected nematodes	https://doi.org/10.3929/ethz-b-000354394	https://www.nature.com/articles/s41586-019-1418-6
			sa_ant_diversity		ant_richness	1	0.0007	The global distribution of known and undiscovered ant biodiversity	≈20 km	No. spp	https://doi.org/10.5061/dryad.wstqjq2pp	https://www.science.org/doi/10.1126/sciadv.abp9908
	0.09242	species_microbes	sm_phylo_diverge		alpha_sespd	50	0.0092	Phylogenetic dispersion of fungal communities	≈1 km	Phylogenetic dispersion (unitless)	https://doi.org/10.5281/zenodo.8013448	https://www.science.org/doi/10.1126/sciadv.adj8016
					alpha_spd	50	0.0092	Phylogenetic diversity of fungal communities	≈1 km	Total phylogenetic branch lengths	https://doi.org/10.5281/zenodo.8013448	https://www.science.org/doi/10.1126/sciadv.adj8016
					beta_b1	50	0.0092	PC1 - Phylogenetic dissimilarity of fungal communities	≈1 km	Phylogenetic dissimilarity (beta	https://doi.org/10.5281/zenodo.8013448	https://www.science.org/doi/10.1126/sciadv.adj8016
					beta_b2	50	0.0092	PC2 - Phylogenetic dissimilarity of fungal communities	≈1 km	Phylogenetic dissimilarity (beta	https://doi.org/10.5281/zenodo.8013448	https://www.science.org/doi/10.1126/sciadv.adj8016
					beta_b3	50	0.0092	PC3 - Phylogenetic dissimilarity of fungal communities	≈1 km	Phylogenetic dissimilarity (beta	https://doi.org/10.5281/zenodo.8013448	https://www.science.org/doi/10.1126/sciadv.adj8016
			sm_richness	sm_alpha_diversity	alpha_ecm	50	0.0058	Richness of ectomycorrhizal fungi	≈1 km	No. of OTUs (alpha diversity)	https://doi.org/10.5281/zenodo.8013448	https://www.science.org/doi/10.1126/sciadv.adj8016
					alpha_am	50	0.0058	Richness of arbuscular mycorrhizal fungi	≈1 km	No. of OTUs (alpha diversity)	https://doi.org/10.5281/zenodo.8013448	https://www.science.org/doi/10.1126/sciadv.adj8016
					alpha_nma	50	0.0058	Richness of non-EcM Agaricomycetes	≈1 km	No. of OTUs (alpha diversity)	https://doi.org/10.5281/zenodo.8013448	https://www.science.org/doi/10.1126/sciadv.adj8016
					alpha_mold	50	0.0058	Richness of molds	≈1 km	No. of OTUs (alpha diversity)	https://doi.org/10.5281/zenodo.8013448	https://www.science.org/doi/10.1126/sciadv.adj8016
					alpha_ohp	50	0.0058	Richness of opportunistic human parasitic fungi	≈1 km	No. of OTUs (alpha diversity)	https://doi.org/10.5281/zenodo.8013448	https://www.science.org/doi/10.1126/sciadv.adj8016
					alpha_path	50	0.0058	Richness of putative pathogenic fungi	≈1 km	No. of OTUs (alpha diversity)	https://doi.org/10.5281/zenodo.8013448	https://www.science.org/doi/10.1126/sciadv.adj8016
					alpha_ucel	50	0.0058	Richness of unicellular, non-yeast fungi	≈1 km	No. of OTUs (alpha diversity)	https://doi.org/10.5281/zenodo.8013448	https://www.science.org/doi/10.1126/sciadv.adj8016
					alpha_yeast	50	0.0058	Richness of yeasts	≈1 km	No. of OTUs (alpha diversity)	https://doi.org/10.5281/zenodo.8013448	https://www.science.org/doi/10.1126/sciadv.adj8016
	0.16636	species_plants	sp_phylo_fun	sp_phylo_diverge	pazfundiverge	1	0.0005	Functional_Divergence_PazEtAl	≈100 km	Functional divergence index, RaoQ	https://doi.org/10.5061/dryad.h9w0vt4rx	https://doi.org/10.1111/geb.13877
					pazphydiverge	1	0.0005	Phylogenetic_Divergence_PazEtAl	≈100 km	Mean pairwise distance	https://doi.org/10.5061/dryad.h9w0vt4rx	https://doi.org/10.1111/geb.13877
				sp_phylo_diversity	pazfundiverse	1	0.0005	Functional_Diversity_PazEtAl	≈100 km	Functional richness index, FRic	https://doi.org/10.5061/dryad.h9w0vt4rx	https://doi.org/10.1111/geb.13877
					pazphydiverse	1	0.0005	Phylogenetic_Diversity_PazEtAl	≈100 km	Faith's phylogenetic diversity	https://doi.org/10.5061/dryad.h9w0vt4rx	https://doi.org/10.1111/geb.13877
			sp_richness	sp_alpha_diversity	sabatini	90	0.0644	Vascular plant alpha diversity for plots of 1000m2 size (Sabatini et al. 2022)	≈1 km	No. spp	https://idata.idiv.de/ddm/Data/ShowData/3506?version=70	https://doi.org/10.1038/s41467-022-32063-z
				sp_gamma_diversity	giftrich	90	0.0252	Gamma diversity using the GIFT database	≈88 km	No. spp (gamma diversity, i.e., total	https://gift.uni-goettingen.de/shiny/predictions/	https://nph.onlinelibrary.wiley.com/doi/10.1111/nph.18533
					kraftsr	90	0.0252	Kraft_Jetz Combined Species Richness	≈110 km	No. spp (gamma diversity)	https://doi.org/10.1073/pnas.0608361104	https://doi.org/10.1073/pnas.0608361104
				sp_anthro_impacts	asi_n_ellis	50	0.0119	[ASI = Anthropogenic Species Increase = IS + CS + OS] / [N = Native Species Richness (based on Kreft & Jetz 2007)]	≈88 km	No. spp	https://anthroecology.org/anthromes/plantbiodiversity/maps	https://doi.org/10.1371/journal.pone.0030535
					asl_n_ellis	50	0.0119	[ASL = Anthropogenic Species Loss] / [N = Native Species Richness (based on Kreft & Jetz 2007)]	≈88 km	No. spp	https://anthroecology.org/anthromes/plantbiodiversity/maps	https://doi.org/10.1371/journal.pone.0030535
					is_n_ellis	50	0.0119	[IS = Species Invasions (based on Lonsdale 1999)] / [N = Native Species Richness (based on Kreft & Jetz 2007)]	≈88 km	No. spp	https://anthroecology.org/anthromes/plantbiodiversity/maps	https://doi.org/10.1371/journal.pone.0030535
					asr_n_ellis	50	0.0140	[ASR = Anthropogenic Species Richness = N - ASL + ASI] / [N = Native Species Richness (based on Kreft & Jetz 2007)]	≈88 km	No. spp	https://anthroecology.org/anthromes/plantbiodiversity/maps	https://doi.org/10.1371/journal.pone.0030535

4. Comparison with similar global indices

To compare SEED with three of the most widely used global indices, we computed the difference between SEED and the MSA from GLOBIO[86], the BII from the Natural History Museum[114], and a second BII (which we will call BDI) produced with a less recent version of the same core methodology[84,115]. The broad scale differences in our index indicate that SEED may be more conservative than MSA and BII (Figure S2a-b) in boreal and desert regions, while SEED estimates higher intactness across temperate regions, sub-Saharan Africa, South Africa, and parts of Australia (Figure S2a-b). SEED was consistently lower than the BDI globally (Figure S2c). Underlying these differences, the distribution of MSA and BII values are bimodal compared with the BDI and SEED, which are unimodal. This means that MSA and BII may more commonly characterize an ecosystem as either highly intact or not very intact, while SEED would more commonly characterize the same ecosystem as moderately intact.

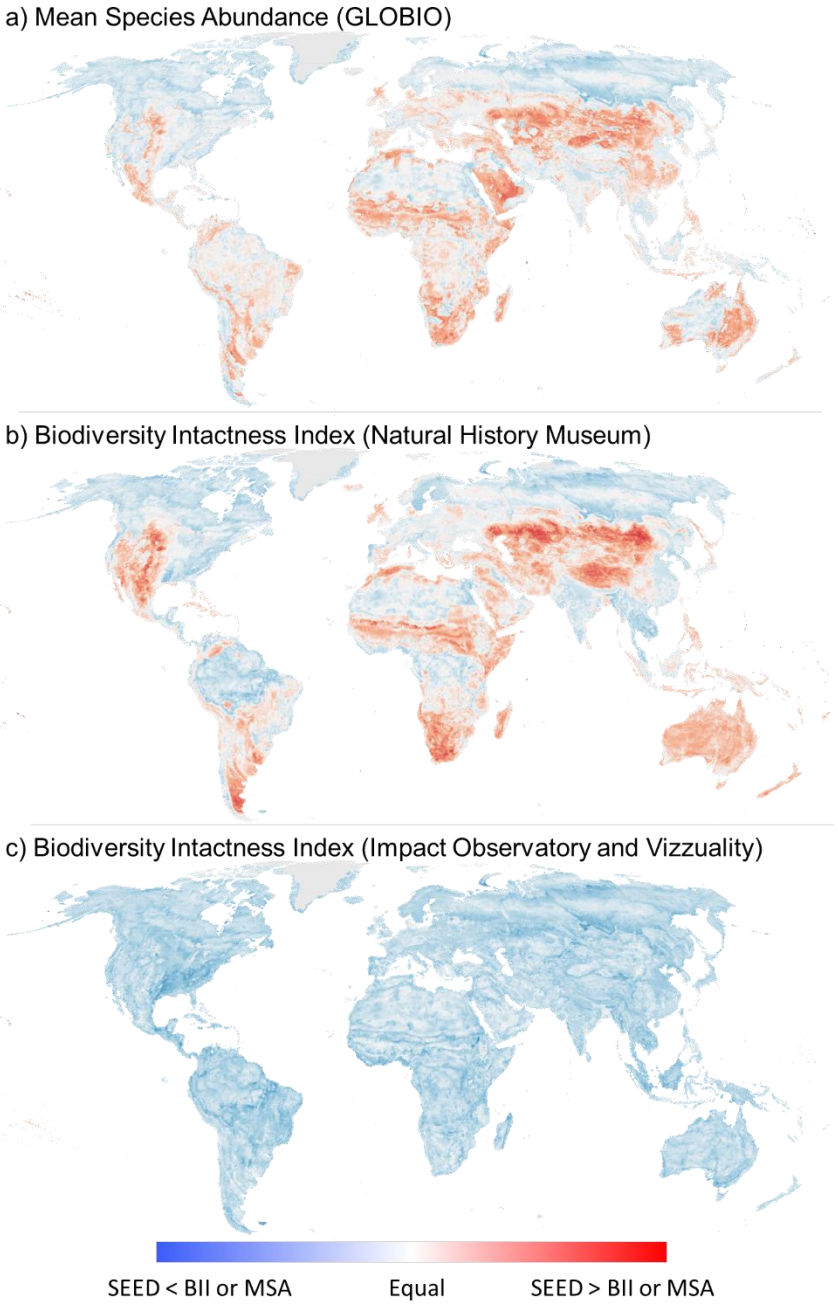

998

999 **Figure S2. Comparison between the leading global biodiversity models.** These global maps
1000 illustrate differences between SEED and (a) MSA[86], (b) BII from NHM[114], and (c) BDI, which was
1001 created independently from the BII while using the same model[115].